SDAC-TR-78-11



# SOME ASPECTS OF Lg AND Pg PROPAGATION

Zoltan A. Der, Charmaine P. Mrazek, Eugene Smart, and B.W. Barker
Seismic Data Analysis Center
Teledyne Geotech, 314 Montgomery Street, Alexandria Virginia 22314



19 March 79



Sponsored by
The Defense Advanced Research Projects Agency (DARPA)
DARPA Order No. 2551

Monitored By
AFTAC/VSC
312 Montgomery Street, Alexandria, Virginia 22314

Disclaimer: Neither the Defense Advanced Research Projects Agency nor the Air Force Technical Applications Center will be responsible for information contained herein which has been supplied by other organizations or contractors, and this document is subject to later revision as may be necessary. The views and conclusions presented are those of the authors and should not be interpreted as necessarily representing the official policies, either expressed or implied, of the Defense Advanced Research Projects Agency, the Air Force Technical Applications Center, or the US Government.

Unclassified

SECURITY CLASSIFICATION OF THIS PAGE (When Data Entered)

## REPORT DOCUMENTATION PAGE

READ INSTRUCTIONS BEFORE COMPLETING FORM

(14) 1. REPORT NUMBER: SDAC-TR-78-11

2. GOVT ACCESSION NO.: AD-A094890

3. RECIPIENT'S CATALOG NUMBER:

4. TITLE (and Subtitle): (6) SOME ASPECTS OF $L_g$ AND $P_g$ PROPAGATION.

5. TYPE OF REPORT & PERIOD COVERED: (9) Technical rept.

6. PERFORMING ORG. REPORT NUMBER:

7. AUTHOR(s): (10) Zoltan A. Der, B. W. Barker, Charmaine P. Mrazek, Eugene Smart

8. CONTRACT OR GRANT NUMBER(s): (15) F08606-78-C-0007

9. PERFORMING ORGANIZATION NAME AND ADDRESS:
Teledyne Geotech
314 Montgomery Street
Alexandria, Virginia 22314

10. PROGRAM ELEMENT, PROJECT, TASK AREA & WORK UNIT NUMBERS: DARPA Order-2551 — T/8709/B/PMP

11. CONTROLLING OFFICE NAME AND ADDRESS:
Defense Advanced Research Projects Agency
Nuclear Monitoring Research Office
1400 Wilson Blvd., Arlington, Virginia 22209

12. REPORT DATE: 19 March 79

13. NUMBER OF PAGES: 63

14. MONITORING AGENCY NAME & ADDRESS (if different from Controlling Office):
VELA Seismological Center
312 Montgomery Street
Alexandria, Virginia 22314

15. SECURITY CLASS. (of this report): Unclassified

15a. DECLASSIFICATION/DOWNGRADING SCHEDULE:

16. DISTRIBUTION STATEMENT (of this Report)

APPROVED FOR PUBLIC RELEASE; DISTRIBUTION UNLIMITED.

17. DISTRIBUTION STATEMENT (of the abstract entered in Block 20, if different from Report)

18. SUPPLEMENTARY NOTES

Author's Report Date 10/22/78

19. KEY WORDS (Continue on reverse side if necessary and identify by block number)

$L_g$ Phase — Crustal Phases

$P_g$ or $\bar{P}$ Phase

20. ABSTRACT (Continue on reverse side if necessary and identify by block number)

$L_g$ and $P_g$ ($\bar{P}$) wavetrains consist of S and P waves trapped in the continental crust. The modal structure of these waves can be approximated from raytracing and Brune's (1964) constructive interference criteria for normal modes. Ray theory arguments show that the modes involved in $L_g$ and $P_g$ propagation are extremely sensitive to internal random inhomogeneities in the crust and small deviations of the free surface or the Moho from plane parallel surfaces.

DD FORM 1 JAN 73 1473 EDITION OF 1 NOV 65 IS OBSOLETE

Unclassified

SECURITY CLASSIFICATION OF THIS PAGE (When Data Entered)

408258

# SOME ASPECTS OF $L_g$ AND $P_g$ PROPAGATION

SEISMIC DATA ANALYSIS CENTER REPORT NO.: SDAC-TR-78-11

| | |
|---|---|
| AFTAC Project Authorization No.: | VELA T/8709/B/PMP |
| Project Title: | Seismic Data Analysis Center |
| ARPA Order No.: | 2551 |
| Name of Contractor: | TELEDYNE GEOTECH |
| Contract No.: | F08606-78-C-0007 |
| Date of Contract: | 01 October 1977 |
| Amount of Contract: | $2,674,245 |
| Contract Expiration Date: | 30 September 1978 |
| Project Manager: | Robert R. Blandford<br>(703) 836-3882 |

P. O. Box 334, Alexandria, Virginia 22313

**APPROVED FOR PUBLIC RELEASE; DISTRIBUTION UNLIMITED.**

Erratum

(Report SDAC-TR-78-11)

Equation 1 should read

$$2N = (2t - \Delta/c)\frac{1}{T} + \frac{1}{2} \qquad (1)$$

On page 14

the correct text is

"The 1/2 in the formula accounts for a $\pi/2$ phase shift..."

PLEASE ENCLOSE WITH ALL
COPIES OF THE REPORT

Z. A. Der

ABSTRACT

$L_g$ and $P_g$ ($\overline{P}$) wavetrains consist of S and P waves trapped in the continental crust. The modal structure of these waves can be approximated from ray-tracing and Brune's (1964) constructive interference criteria for normal modes. Ray theory arguments show that the modes involved in $L_g$ and $P_g$ propagation are extremely sensitive to internal random inhomogeneities in the crust and small deviations of the free surface or the Moho from plane parallel surfaces.

TABLE OF CONTENTS

LIST OF FIGURES

LIST OF FIGURES (Continued)

LIST OF TABLES

## INTRODUCTION

This report, which should be considered a progress report, summarizes portions of the continuing research done to date on regional phases at the Seismic Data Analysis Center (SDAC). Some of the results and computer programs developed will be used in the just initiated array design and processing study. This phase of the study is aimed at exploring the nature of two types of signals to be processed ($P_g$ ($\overline{P}$) and $L_g$) and to outline some limitations of the modal approach. While most arguments are heuristic in nature, using gross approximations, the authors think conclusions reached here can be justified and that even more exact analysis will not invalidate them.

Most crustal phases are considered a subset of guided waves that can exist in the earth. Any major velocity gradient can act as the boundary of a waveguide: the 400 km discontinuity traps the body waves which make up the $P_a$ and $S_a$ phases (Schwab, Kausel, and Knopoff, 1974), the lithospheric plate boundary at about 100 km guides the $S_n$ wave, and the Mohorovic discontinuity which marks the bottom of the crust traps the $P_g$ and $L_g$ phases. These phases or guided waves will exist only insofar as their waveguide remains intact; thus, the $P_a$ and $S_a$ phases propagate through continents and oceans because the 400 km discontinuity exists everywhere, while $L_g$ is interrupted by the ocean-continent boundaries because the continental waveguide terminates there.

In this report we examine two regional phases, $L_g$ and $P_g$ (or $\overline{P}$), as they appear on the short period instruments.

### Ray Theory Approximations to $L_g$ and $P_g$

$L_g$ is a high frequency phase entirely confined to propagation in a continental crust (Press and Ewing, 1952). The $L_g$ phase arrives ahead of the

Schwab, F., E. Kausel and L Knopoff, 1974, Interpretations of $S_a$ for a shield structure; Geophys. J. R. Astr. Soc., 36, 737.

Press, F. and M. Ewing, 1952, Two slow surface waves across North America; Bull. Seism. Soc. Am., 43, 219.

fundamental mode surface waves and the arrival is apparent on all three components: vertical, radial and transverse. It also involves both SH and P-SV waves, and the frequencies are considerably higher than in the fundamental mode, mostly in the .1 - 1.5 Hz range. Some workers have interpreted $L_g$ as a superposition of Airy phases of higher continental Love and Rayleigh modes (Knopoff, Schwab and Kausel, 1973; Panza and Calcagnile, 1975). Frequency content and group velocities of waves in the $L_g$ wave train support this interpretation. Closer inspection of $L_g$ reveals sudden increases of amplitudes at certain times, "phases" in $L_g$, variously named by workers. The "phases" of $L_g$ are probably associated with minima in group velocity (Airy phases) of some prominent modes (Knopoff, Schwab, Nakanishi and Chang, 1974; Panza and Calcagnile, 1975). Synthetic seismograms, computed by adding surface wave normal modes, exhibit many features of actual seismograms and show convincingly that $L_g$ might well be composed of higher mode surface waves. Figure 1 shows Love wave phase and group velocity for a continental shield type of crustal model (drawn after Knopoff, Schwab and Kausel, 1973).

The strikingly regular spacing of higher mode phase velocity curves and the sudden change of slopes around 4.7 km sec (subcrustal shear wave velocity) suggest that the phase velocities of various modes are interrelated, and that the sudden change in slopes must stem from trapping SH waves in the crust. A similar regularity appears in Rayleigh (SV-P type) wave (Figure 2 from Panza and Calcagnile) phase velocity curves for a somewhat different model. This regular behavior suggests a simple relationship between modes, such as Brune's (1964, 1966) constructive interference criterion as applied to the travel times


Knopoff, L., F. Schwab and E. Kausel, 1973, Interpretation of $L_g$; Geophys. J. R. Astr. Soc., 33, 389.

Panza, G. F. and G. Calcagnile, 1975, $L_g$, $L_i$ and $R_g$ from Rayleigh modes; Geophys. J. R. Astr. Soc., 40, 475.

Knopoff, L., F. Schwab, K. Nakanishi and F. Chang, 1974, Evaluation of $L_g$ as a discriminant among different continental crustal structures; Geophys. J. R. Astr. Soc., 26, 255.

Brune, J. N., 1964, Travel times, body waves and normal modes of the Earth; Bull. Seism. Soc. Am., 54, 2099-2128.

Brune, J. N., 1966, P and SV wave travel times and spheroidal normal modes of homogeneous spheres; J. Geophys. Res., 71, 2959.

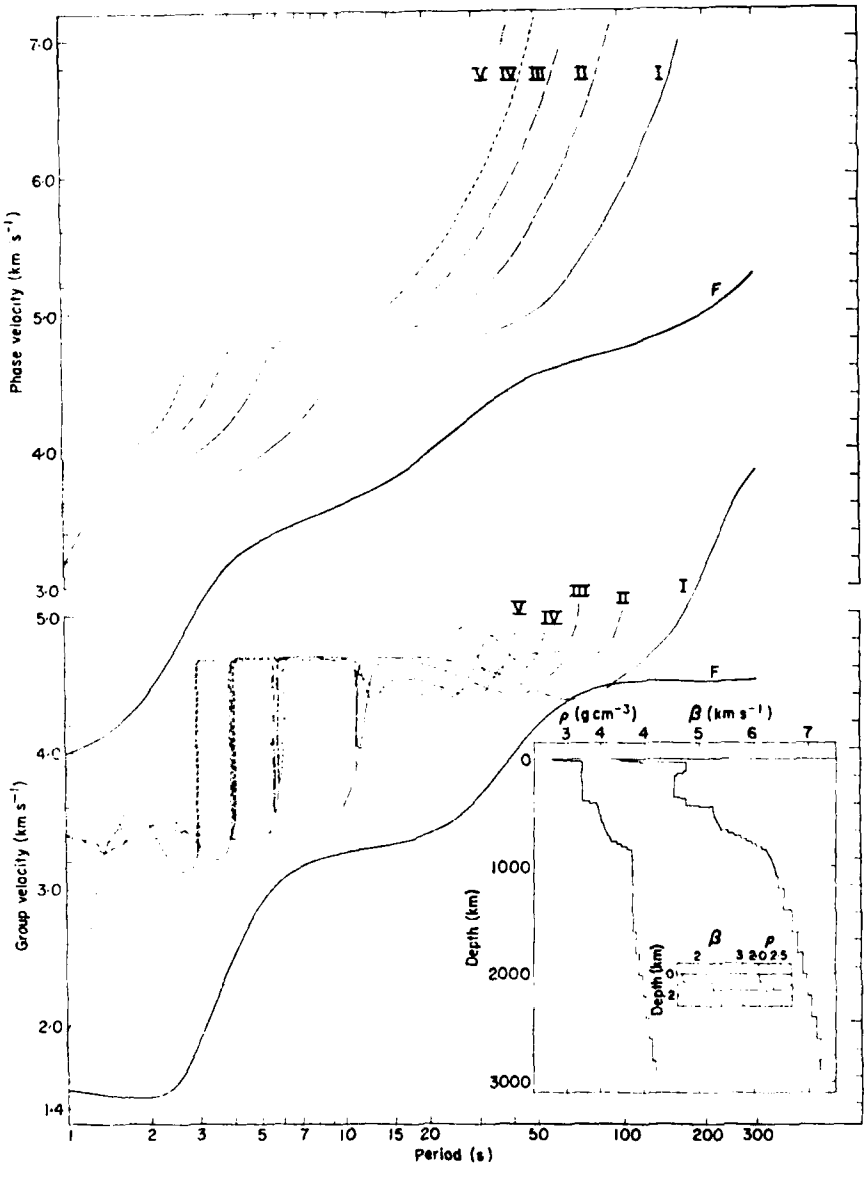


Figure 1. Phase and group velocity curves of the fundamental and first five higher Love modes in a shield type continental crust (after Knopoff, Schwab and Kausel, 1973).

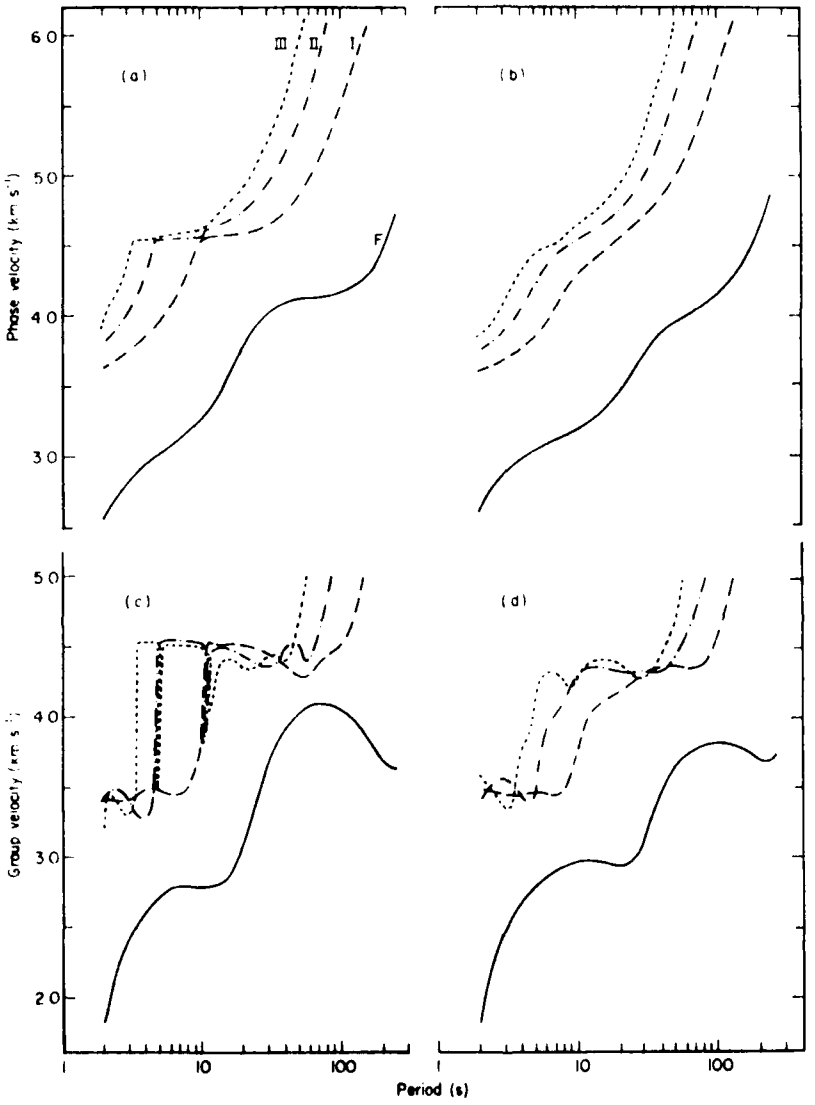


Figure 2. Phase and group velocity curves of the fundamental and first three higher Rayleigh modes in a shield type continental crust (after Panza and Calcagnile, 1975).

obtained from ray tracing. One could ray trace through the same model used for model calculations and then find phase velocities which give constructive interference at a certain period, distance and travel time. Inspecting the depth dependence of the particle motion of various modes at the minima of group velocity further confirms this notion (Figures 3 and 4).

All depth versus displacement curves have maxima at the free surface, various numbers of nulls in the crust, and they decay exponentially below the Moho. This particle motion pattern can result from interference of up and downgoing shear waves trapped in the crust. The amplitude depth curves of higher mode surface waves, confined to the other waveguides mentioned above, are essentially similar because they have many zero crossings (nulls) terminated by an exponential decrease below the interface in question. This is true for both Rayleigh and Love type modes.

Now, using ray theory, we will attempt to reconstruct some of the major features of the propagation and excitation of $L_g$ and $P_g$. Although modal and ray theory representation of propagation phenomena ought to be equivalent, at least in the high frequency limit (Ben-Menahem, 1964), examining the ray theory aspects of the crustal phases $L_g$ and $P_g$ provides some physical insight into the limitations of the modal approach not readily apparent in the implicit formulation of modal calculations.

At first, we tried to apply Brune's (1964) constructive interference criterion to travel times computed using ray tracing through Harkrider's shield model, which Knopoff had used for his Love mode calculation. We utilized TVT2, Julian's computer program, to do the raytracing (Julian and Anderson, 1968). Brune's constructive interference criterion can be written as

$$2N = (2t - \Lambda/c)\,\frac{1}{T} + \frac{\pi}{2} \qquad (1)$$

Ben-Menahem, A., 1964, Mode-ray duality; Bull. Seism. Soc. Am., 54, 1315.

Julian, Bruce R. and Don L. Anderson, 1968, Travel times apparent velocities and amplitudes of body waves; Bull. Seism. Soc. Am., 58, 339.

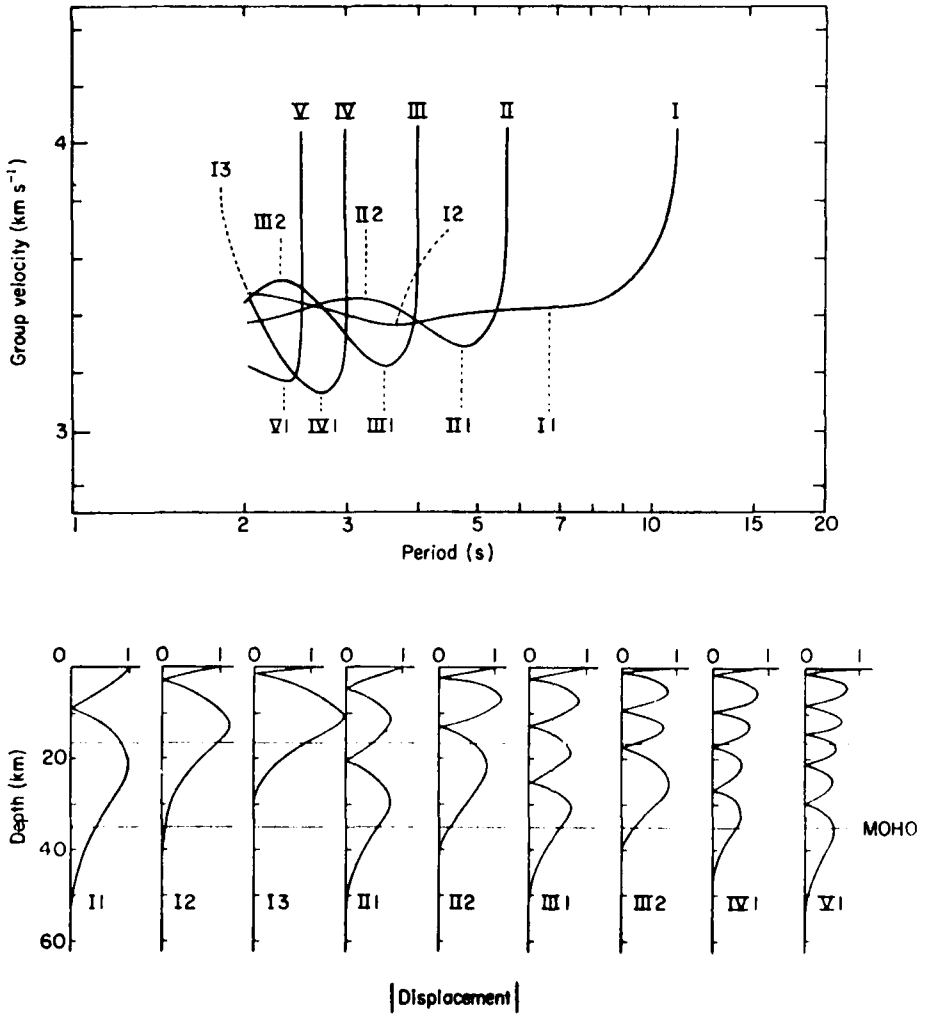


Figure 3. Specification of $L_g$ stationary phases and the associated displacment-depth functions of five higher Love modes (after Knopoff, Schwab and Kausel, 1973).

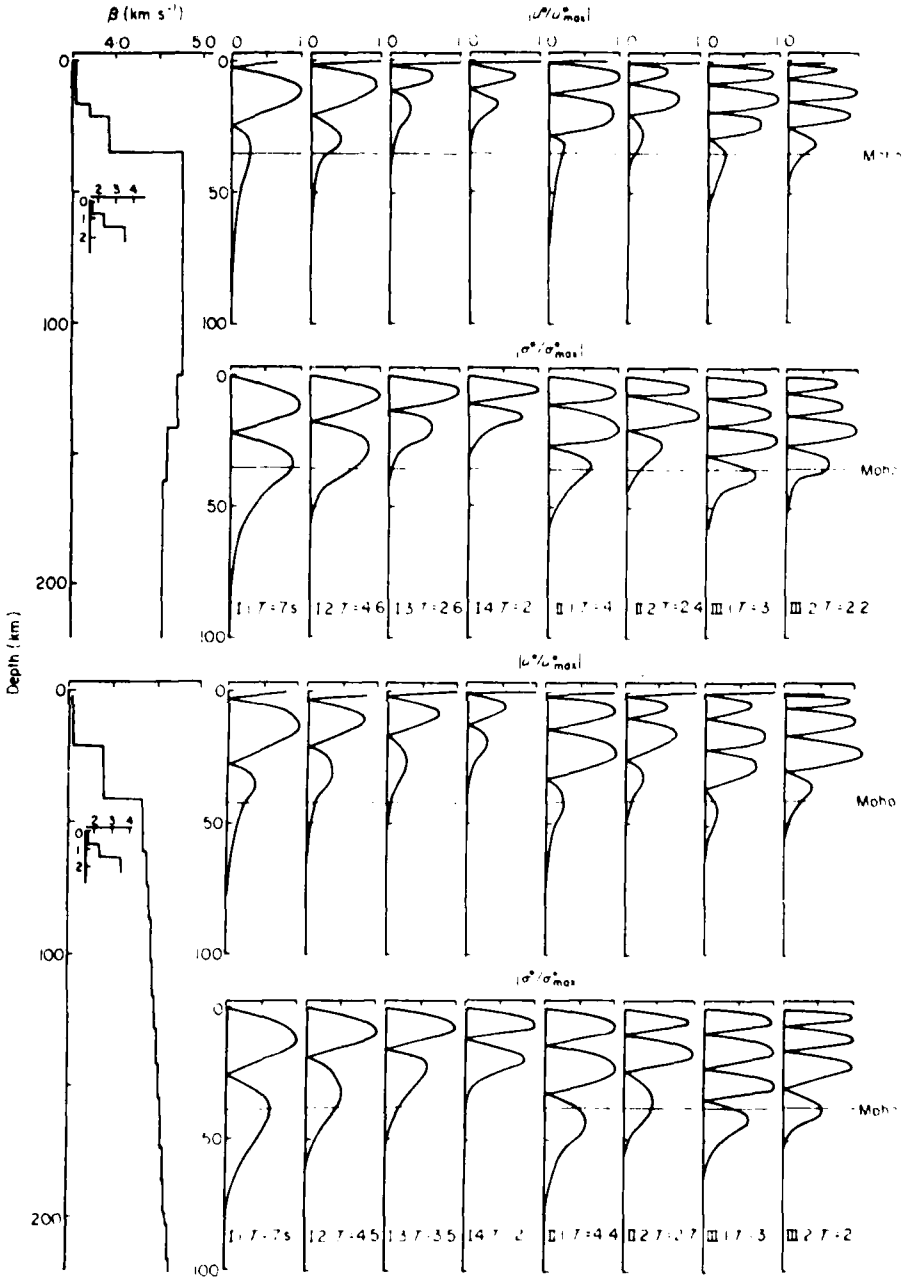


Figure 4. Displacement-depth functions for various stationary phases of higher Rayleigh modes (after Panza and Calcagnile, 1975).

where N is an integer, t is travel time along a diving ray, $c = \frac{d\Delta}{dt}$ is the phase velocity of the ray and T is the wave period. Taking $\Delta$, c, and t for various rays and solving (1) for T, the phase velocity curve of a certain mode can be traced out. Changing N changes the mode number. The $\pi/2$ in the formula accounts for a $\pi/2$ phase shift at the turning point which should be true at the high frequency limit (Tolstoy and Clay, 1966). However, this term may only be valid for the higher mode numbers. Formula 1 assumes no losses from internal reflections and total reflection at the surface.

Note that the expression $(t - \Delta/c)$ is the "new datum" $(t - \frac{dt}{d\Delta})$, which Johnson and Gilbert (1972) proposed for inverting travel time data; it unfolds the triplications of travel time curves yielding a monotonic, integrable function for easy inversion (Bessonova et al., 1974). Thus, apparently, when inverting surface wave data we are actually doing inversions with the quantity $t - p\Delta$, and the various modes and body wave data contain the same information. Because $t - p\Delta$ has jumps at low velocity zones (LVZ), it lacks details of the low velocity zone; this uncertainty also affects surface wave inversion. The same limitation is stated somewhat differently by Panza, Schwab, and Knopoff (1972), who point out that waves prominent in a LVZ are generally not at all - or at best poorly - excited at the surface. Thus, even when using the inversion theory of Backus and Gilbert (1970), the resolution of any detail in a LVZ from real surface wave data may not be as good as a formalistic manipulation of partial derivatives suggests. This result stems from the low amplitudes at the surface of the surface wave period ranges which are most sensitive to the LVZ material properties.

Tolstoy, I. and C. S. Clay, 1966, Ocean Acoustics: New York McGraw-Hill Book Co.

Johnson, L. E. and F. Gilbert, 1972, A new datum for use in the body wave travel time inverse problem; Geophys. J. R. Astr. Soc., 30, 373.

Bessonova, E. N., V. M. Fishman, V. Z. Ryoboyi, G. A. Sitnikova, 1974, The tau method for inversion of travel times - I, Deep seismic sounding data; Geophys. J. R. Astr. Soc., 36, 377.

Panza, G. F., F. Schwab, and L. Knopoff, 1972, Crustal and channel Rayleigh waves; Geophys. J. R. Astr. Soc., 30, 273.

Backus, G. E. and J. F. Gilbert, 1970, Uniqueness in the inversion of gross earth data; Phil. Trans. R. Soc. Lond., No. 266, 123.

We have taken the crustal model of Knopoff, Schwab and Kausel (1973), listed in Table I, and used Julian's ray tracing program to determine travel time curves for both P and S waves for this model. The reduced travel time curves for these models are given in Figures 5 and 6.

Figure 7 presents curves of phase velocity versus period derived from the S wave travel times using Brune's equation (1). The first curve on the right corresponds to the first higher mode of Love waves. Note the visual similarity to the curves of Knopoff et al. (1974) (Figure 1).

The phase velocity curves have several sudden curvature changes that correspond to major velocity discontinuities in the model: the change at 4.7 km/sec corresponds to the Moho and the change at 3.6 km/sec to the top of the intermediate, 15 km thick layer, in the crust. $L_g$ proper occupies the space between the phase velocities 3.5 and 4.7 km/sec. The top two layers of the crust should also act as a waveguide where waves travel at lower group velocities to comprise the tail of the $L_g$ wavetrain. There, lateral inhomogeneities in the upper part of the crust can scatter trapped energy. Thus, the argument (Ruzaikin et al., 1977) that $L_g$ cannot be a superposition of higher modes because the group velocities corresponding to the coda of $L_g$ are low is invalid because while low velocity media exists along the earth's surface some part of the modal curve can always explain low group velocity arrivals. Furthermore, as in the case of fundamental modes, scattered late-arriving waves probably make up much of the coda anyway.

In terms of a waveguide, considerable body wave trapping should develop in the upper crust, where the group velocities are low. However, because the internal structure of the upper-crust is quite variable laterally, these low group velocity waves may be strongly scattered and thus not seen at large distances.

The group velocity curves, corresponding to the approximation $U = \frac{\Delta}{t}$ are shown in Figure 8. Although some similarity to the exact curves exist, the ray approximation is not accurate enough to reproduce the exact mode

---

Ruzaikin, A. I., I. L. Nersesov, V. I. Khatturin and P. Molnar, 1977, Propagation of $L_g$ and lateral variations in crustal structures in Asia; J. Geophys. Res., 82, 307.

TABLE I

Crustal P and S velocity model used in our calculations.

| d (km) | $\alpha$ (km/sec) | $\beta$ (km/sec) |
|---|---|---|
| 1.50 | 4.12 | 2.31 |
| 15.0 | 6.135 | 3.54 |
| 5.0 | 6.41 | 3.70 |
| 13.5 | 6.79 | 3.92 |
| 85.0 | 8.23 | 4.75 |
| 20.0 | 8.15 | 4.70 |
| 20.0 | 7.94 | 4.58 |
| 200.0 | 7.87 | 4.54 |
| 10.0 | 8.05 | 4.643 |
| 65.0 | 8.23 | 4.75 |
| 10.0 | 8.67 | 5.00 |
| 20.0 | 9.10 | 5.25 |
| 40.0 | 9.1 | 5.25 |
| 160.0 | 9.27 | 5.35 |
| 90.0 | 9.97 | 5.75 |
| 90.0 | 10.75 | 6.20 |

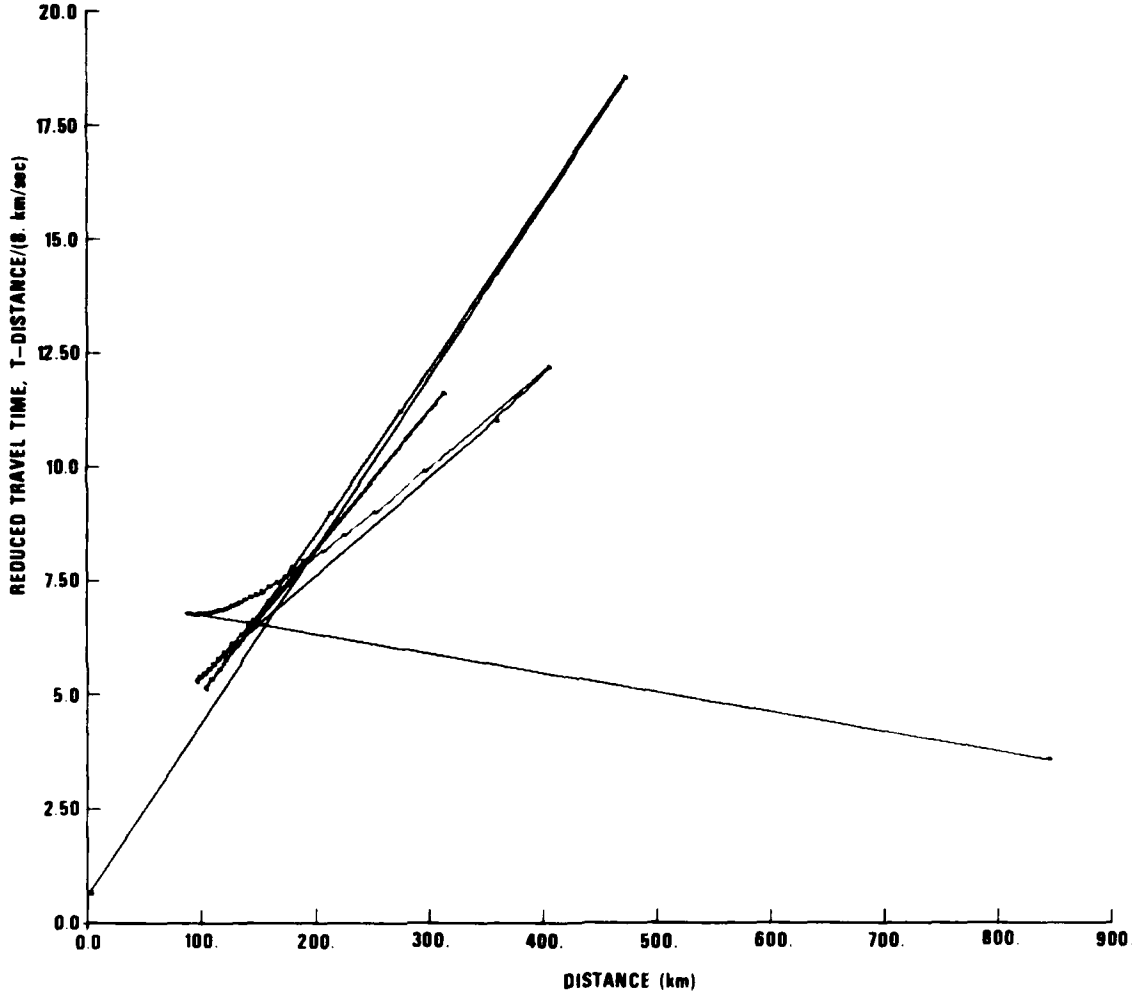


Figure 5. Reduced P wave travel time in the crustal model of Knopoff et al. (1973).

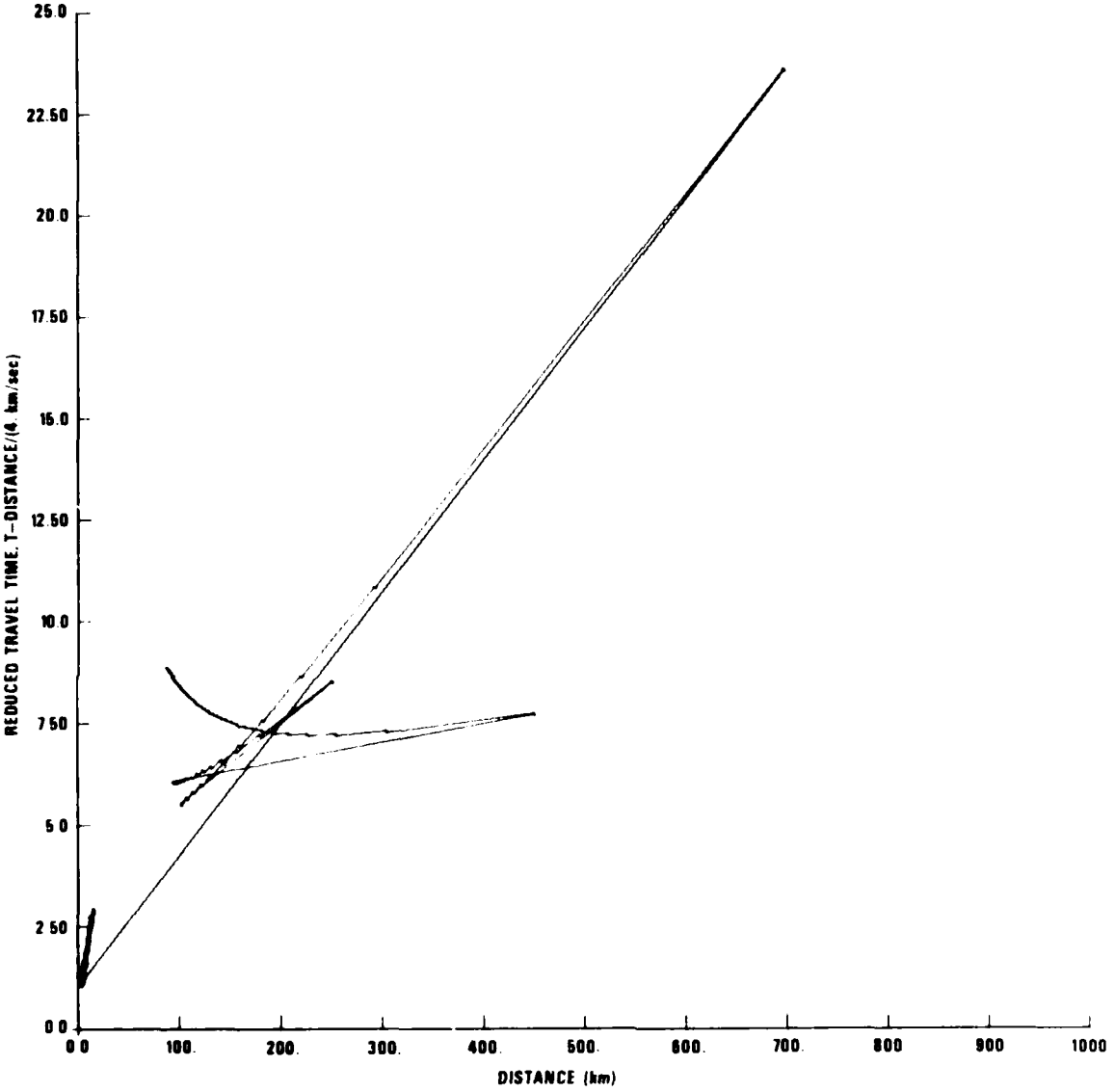


Figure 6. Reduced S wave travel time for the crustal model of Knopoff et al. (1973).

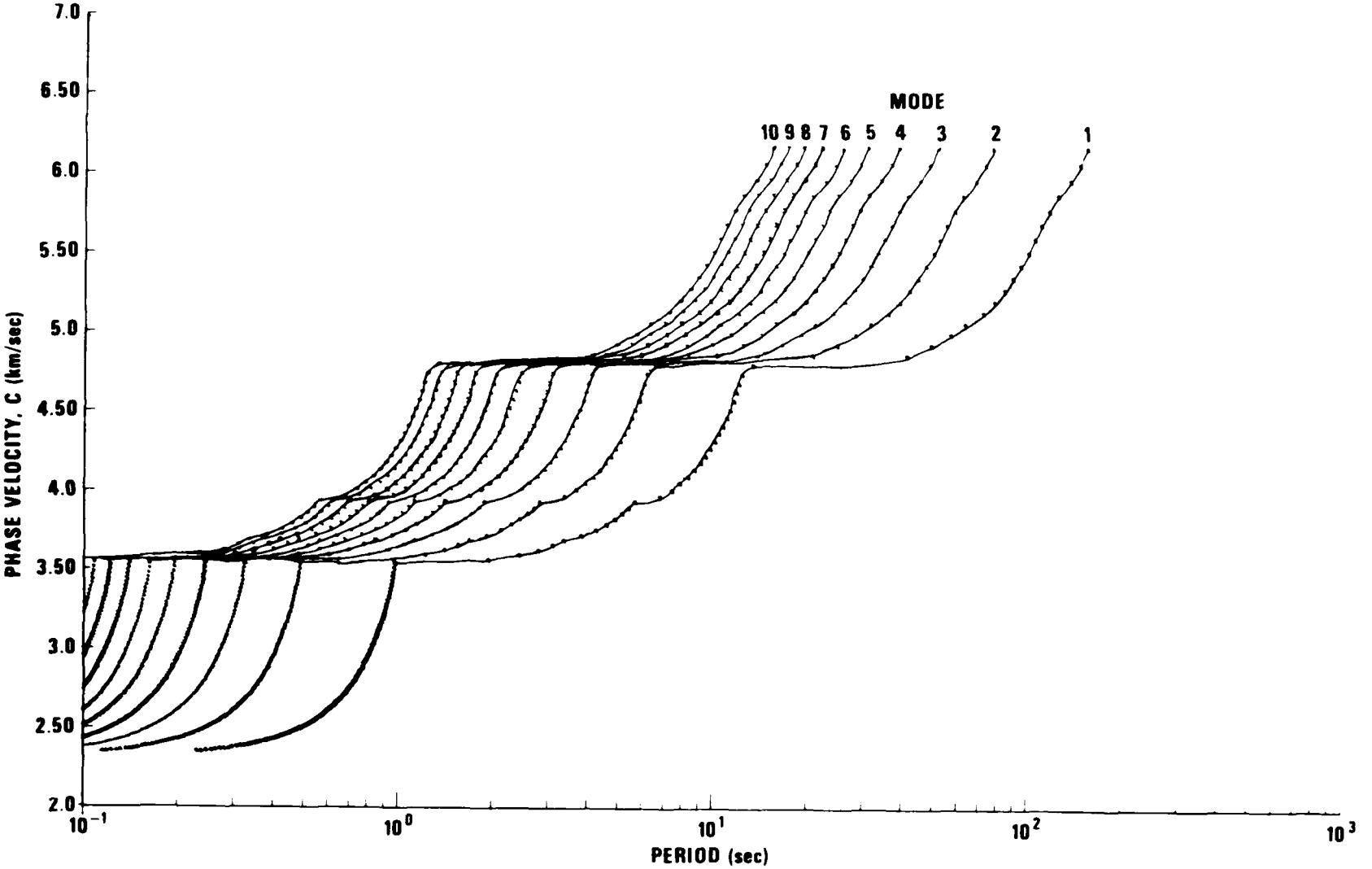


Figure 7. Phase velocity curves for SH waves derived from Brune's constructive interference criteria.

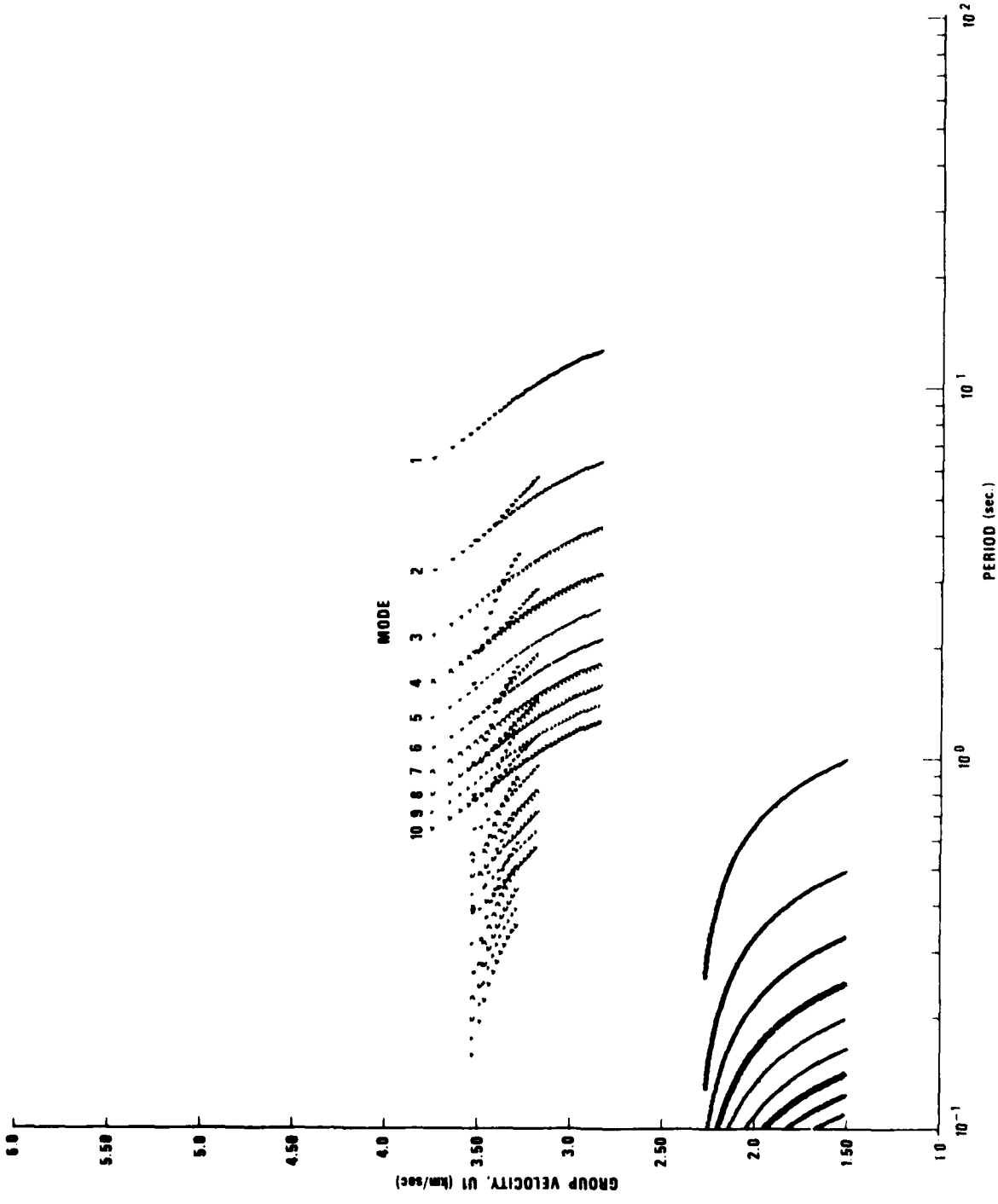


Figure 8. Approximate group velocity curves, U = D/t, for SH waves.

calculation results. Still, the results show considerable concentration of points in the velocity range where $L_g$ should be located. Figure 9 shows some of our phase velocity points plotted on curves from Knopoff et al., (1973). The agreement is fair and it seems to improve, as expected, with mode number.

Panza and Calcagnile (1975) showed that vertical and radial motion in $L_g$ can be explained with higher Rayleigh modes. Rayleigh mode propagation involves P-SV type waves with P-S conversions at major interfaces and the free surface.

Brune (1966) was able to formulate his constructive interference criterion only for a homogeneous sphere, a formulation that accounts for P-SV conversions at the free surface, but not within the sphere. However, because the sharpest velocity contrast is at the free surface, most of the conversions take place there, and, so, Brune's criterion can still be used as an approximation. The surface angles of incidence of the P and S waves that the Moho traps are such that the surface P-S and S-P conversions are almost complete. Using the approximation of complete conversions that occur only at the surface results in a travel path that consists of alternate P and S legs (Figure 10a). The P legs will be much shorter than the SV so, as a further approximation, the P legs can be neglected entirely and Brune's criterion for SV waves used (Figure 10b). This kind of mode is widely known to workers studying spheroidal modes of the earth. Such modes involve mostly SV type motion, with some compressional deformation close to the surface. Results from this approach measure its accuracy; that is, the phase velocities derived with this method are close to those derived exactly (Figure 11). Even though the greatest differences are in the 4.6 - 4.8 km/sec region, the spacing of modes in frequency is still quite similar.

$P_g$ (or more properly $\bar{P}$) is a short period phase with large amplitude, which propagates great distances in the WUS at an average velocity of 6 km/sec. It is regarded as a superposition of higher modes of a "leaky" guided P wave. Haskell (1966) derived phase and group velocities for these modes using a simple one layer crustal model, and, subsequently, a model which also

Haskell, N. A., 1966, The leakage attenuation of continental crustal P waves; J. Geophys. Res., 71, 9355.

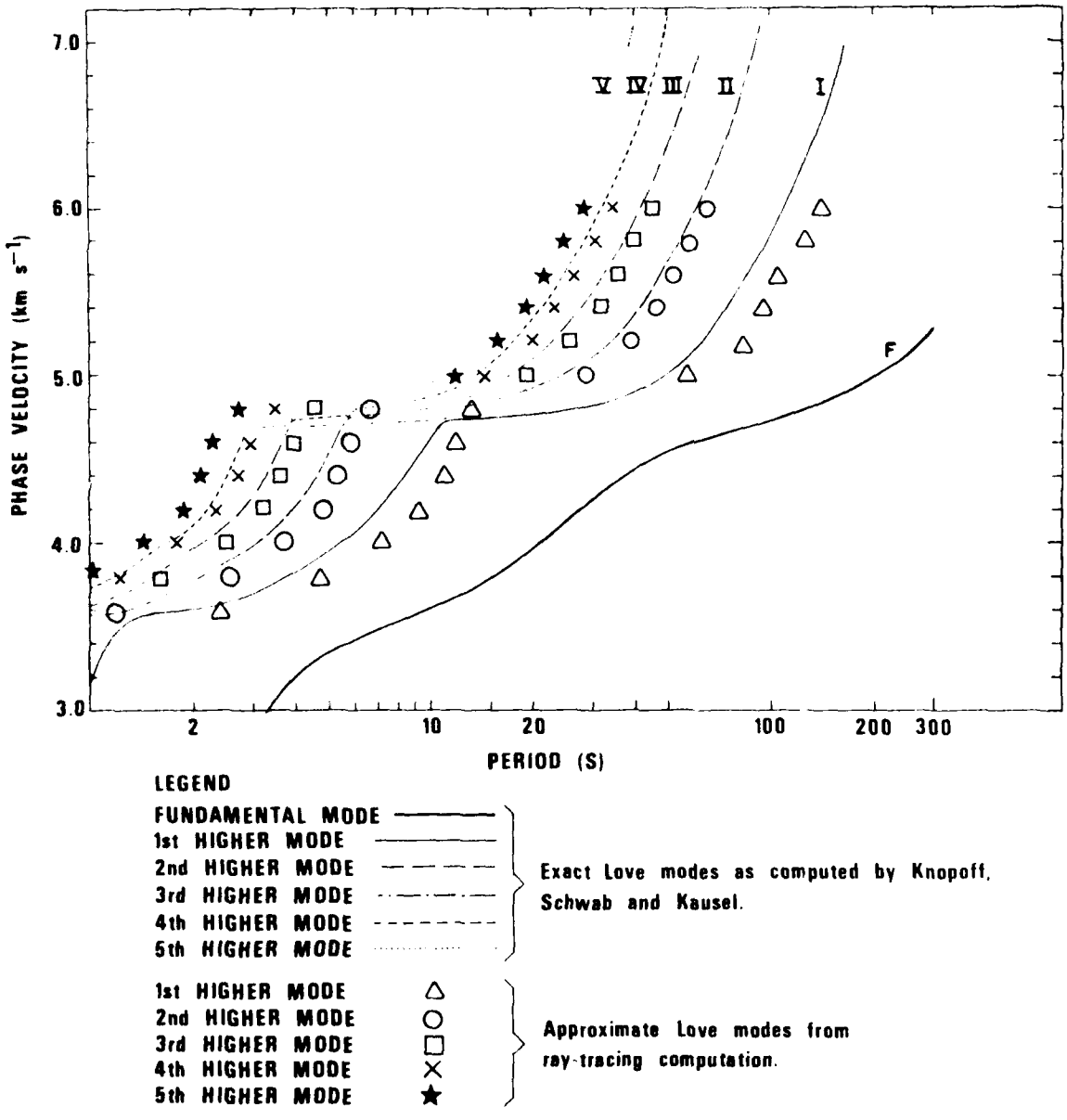


Figure 9. Comparison of exact Love modal phase velocities with those derived from ray approximation.

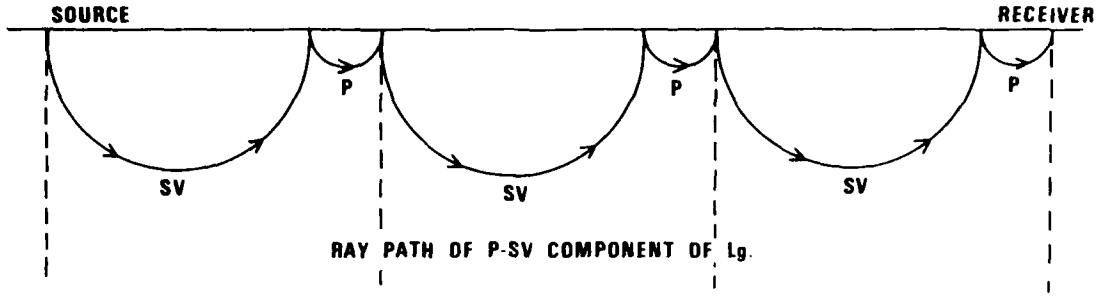


Figure 10a. Approximate mode of the P-SV component of $L_g$.

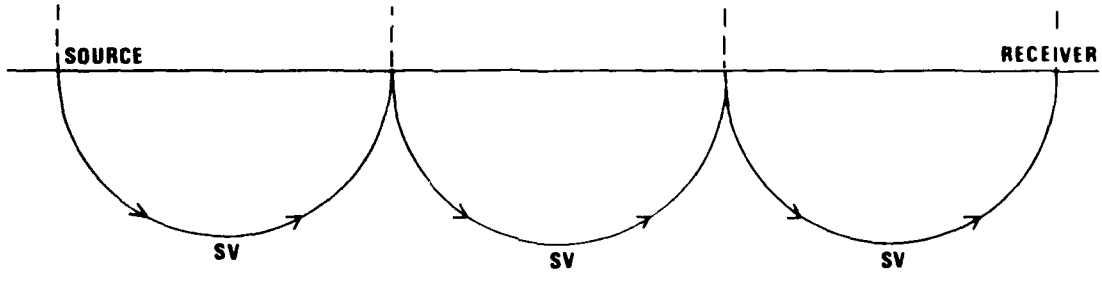


Figure 10b. Approximate ray path diagram, neglecting the P conversions.

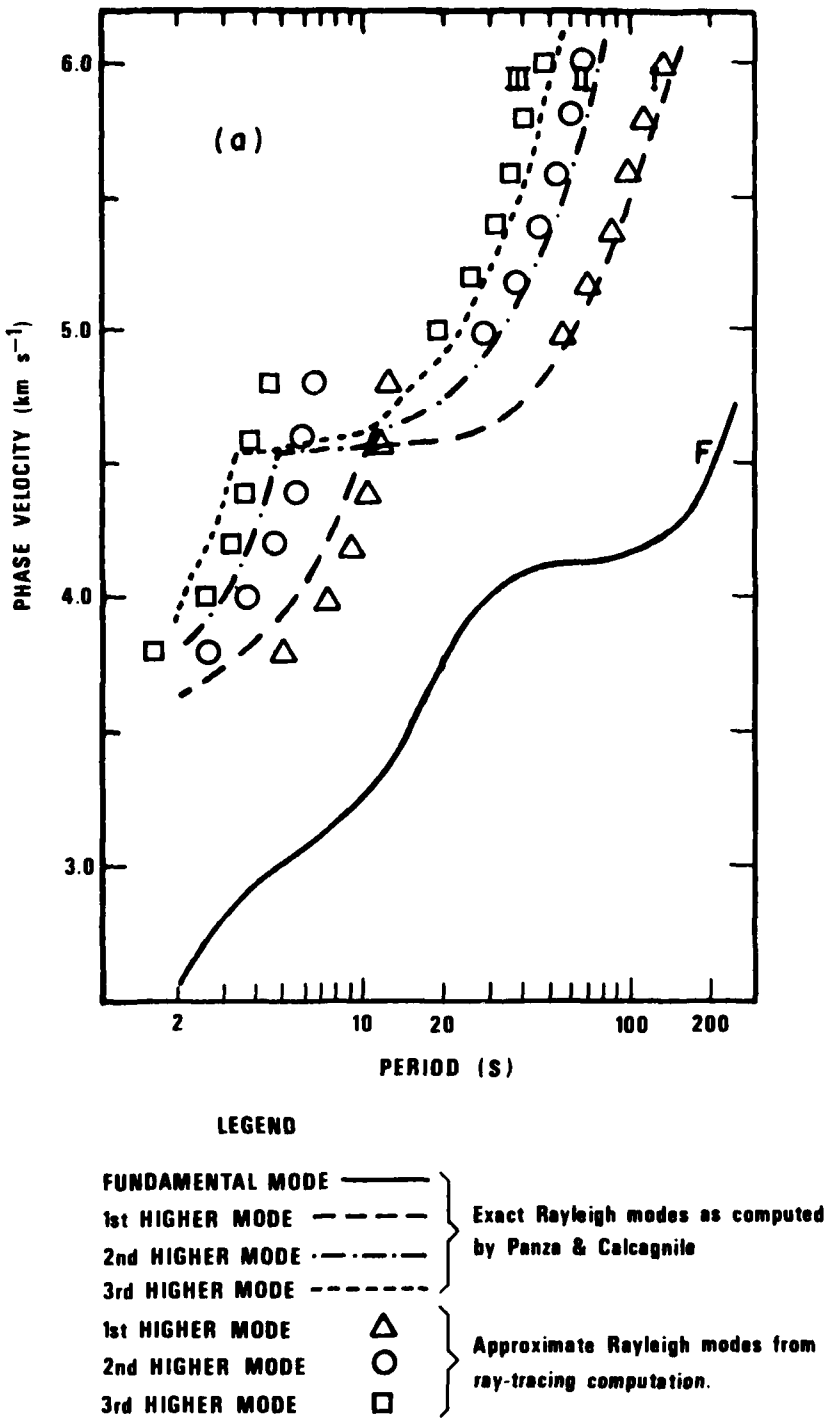


Figure 11. Comparison of exact Rayleigh modal phase velocities with those derived from ray approximation.

included a surface sedimentary layer. By utilizing the P wave travel times in Figure 5 and equation (1), we derived phase velocity curves for these modes similar to Haskell's (Figure 12). The physical model used included P waves constructively interfering in the crust but neglected all S conversions, a process that can be done for some crustal models, usually those with a sedimentary layer at the top. For other models, considerable S conversion and severe attenuation of these modes may occur.

Although the ray methods cannot give fine details of the group velocity structure, they can be used to compute inter-sensor coherence in the direction of propagation. In this case, excitation versus frequency for each mode, and the number and spacing of modes versus frequency is more important than the derived absolute phase velocities. The approximate phase velocity curves and coherences can be calculated rapidly and efficiently. Figure 13 shows inter-sensor coherence curves as functions of sensor spacing in the direction of propagation for $L_g$, indicating that the coherence is still quite high at 2 Hz, despite the presence of about 28 modes. A similar curve for $P_g$ shows that, assuming all other factors equal, spacing of $P_g$ should be more coherent across an array of similar size (Figure 14). These curves can easily be used to compute beaming losses for any modal composition and for various array configurations. These losses can, in turn, be compared to observed rms signal degradation measured for real signals, and the comparison can be used to infer the maximum number of modes present with appreciable energy. Another factor causing decorrelation of signals is multipathing, which can also be modeled using Mack's and Flinn's (1971) azimuthal distribution of arrival directions. One characteristic of such a multipathing model is the dependence of the signal coherence between sensors on the angle between direction of propagation and the line connecting the sensors. The gross correlation properties of $P_g$ and $L_g$ are, therefore, determined by modal composition and multipathing which can be modeled with the methods outlined above.

Mack, H. and E. A. Flinn, 1971, Analysis of the spatial coherence of short-period acoustic gravity waves in the atmosphere; Geophys. J. R. Astr. Soc., 26, 255.

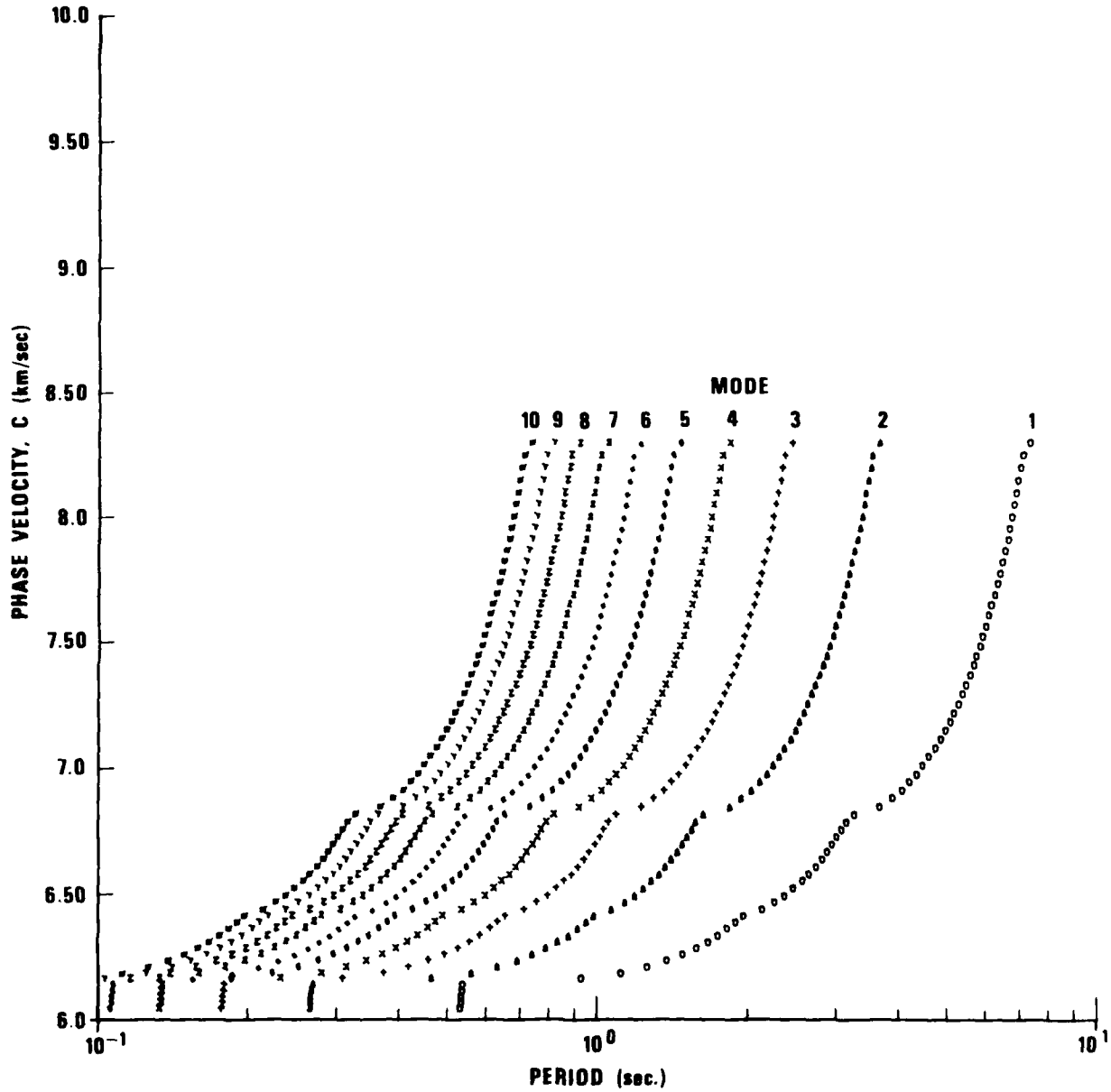


Figure 12. Approximate $P_g$ phase velocity curves derived from ray interference criteria.

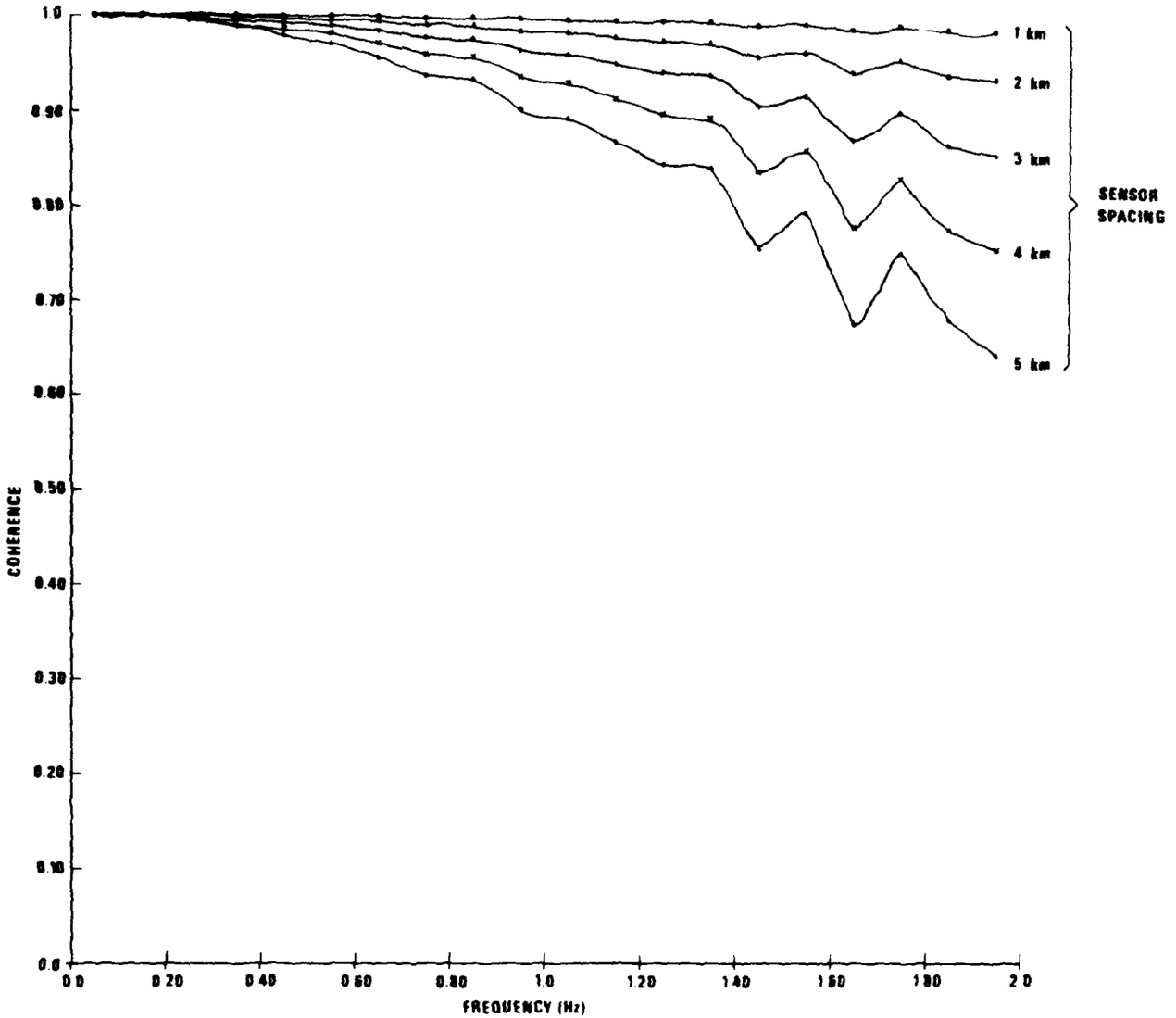


Figure 13. Intersensor coherence of $L_g$ as a function of frequency and intersensor spacing along the lines of propagation.

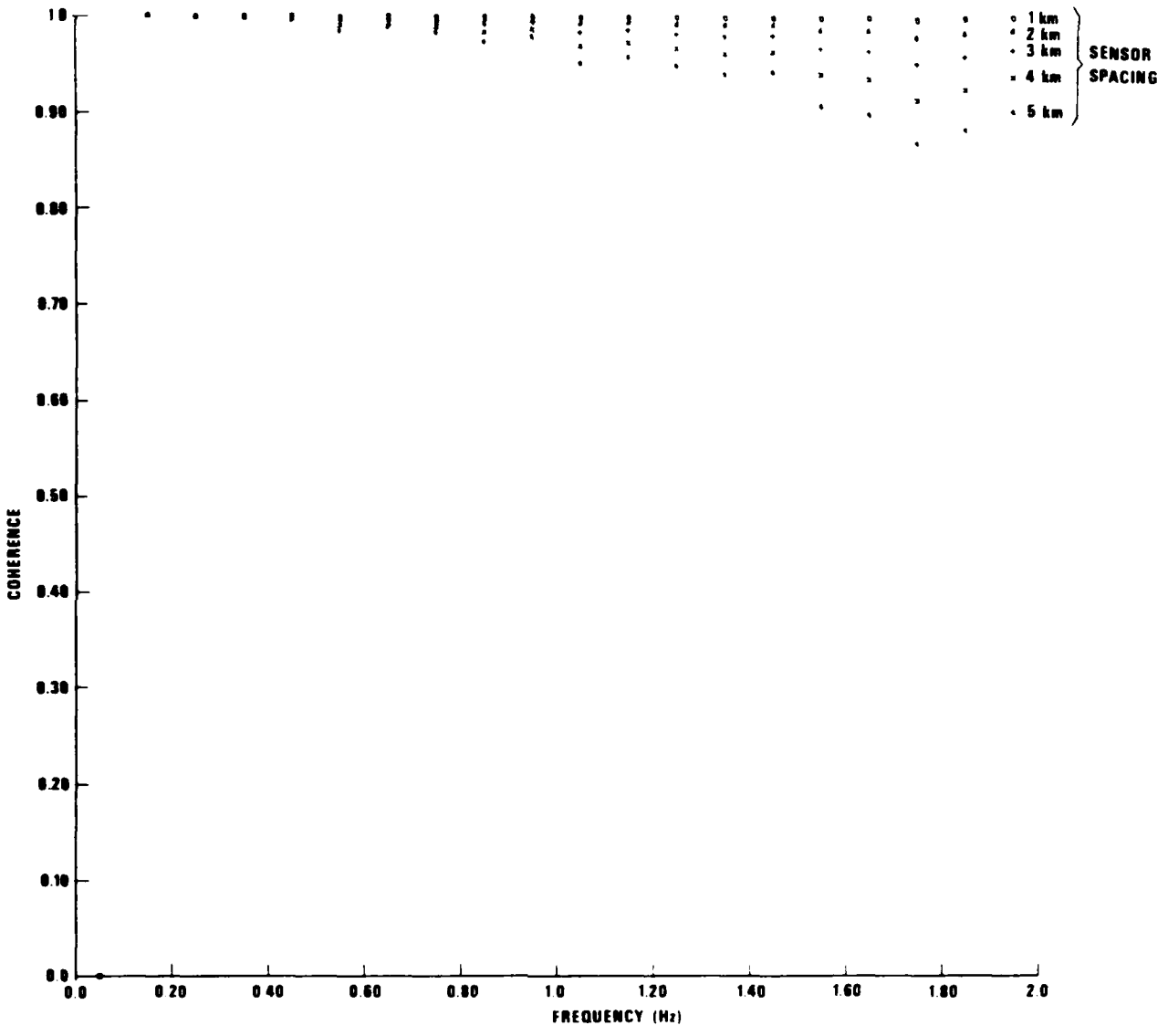


Figure 14. Intersensor coherence of $P_g$.

In the past, other types of theories were also used to simulate $P_g$ and $L_g$. Langston and Helmberger (1974) obtained a $P_g$-like phase using generalized ray theory for a structure between NTS and Tucson. Using asymptotic ray theory, Vered and Ben-Menahem (1977) obtained realistic synthetic seismograms for a path in the Red Sea region. For the case of multiply refracted interfering waves in the crust the results of the generalized and asymptotic ray theories are not expected to differ significantly from simple ray theory.

Effects of Topography and the Randomness of Media

Thus far, this report has shown that the most essential features of higher mode dispersion and excitation can be easily explained using simple ray-type theory. The calculations involving the ray theory, plus interference conditions, are simple and fast when compared to tedious and expensive modal calculations. If ray arguments are used, some basic limitations of the modal theory become apparent. Because the phase velocities of the adjacent modes at the same frequency are similar, any small perturbation in the layered media or a few degrees of slope in the topography or the Moho is sufficient to deflect the energy from one mode into another.

For example, with this model (Knopoff's model A) the average distance between modes in phase velocity at around 1 Hz is about .15 km/sec, which corresponds to a difference in the angle of incidence at the surface of about 1.5 degrees. Thus, a surface slope half that amount at the point of reflection will deflect energy of one mode into the next. Surface slopes of that magnitude are quite common over distances comparable to an $L_g$ 1 Hz wave length, so the modal structure at the high frequencies will probably break down or diffuse. Also, a great part of the apparent attenuation of $L_g$ and $P_g$ is probably unrelated to crustal anelasticity. Part of the energy may be deflected into higher phase velocities by surface (or Moho) topography, then leak into the mantle, and finally become absorbed in the low Q zone there. Another portion may be deflected into the modes trapped in the upper layers

Langston, C. A. and D. V. Helmberger, 1974, Interpretation of body and Rayleigh waves from NTS and Tucson; Bull. Seism. Soc. Am., 64, 1919.

Vered, M. and A. Ben-Menahem, 1974, Application of synthetic seismograms to the study of low magnitude earthquakes in the northern Red Sea region; Bull. Seism. Soc. Am., 64, 1221.

of the crust and then scattered there. Therefore, $L_g$ and $P_g$ will attenuate faster in areas of rugged surface and Moho topography and in areas of upper crustal inhomogeneities.

If various higher modes exchange energy, determining source depth using the nulls of a few modes becomes impossible because all modes may have considerable energy after propagating to a certain distance. Furthermore, the various modes cannot possibly be resolved because of their similarity in phase velocity and frequency content, even after propagating over considerable distances (Knopoff et al., 1974). Despite modal conversions, the energy still propagates locally in a manner of modes where the multiply reflected-refracted waves in the crust reinforce each other according to equation (1).

The ray theory formulation (1) is also beneficial because by disturbing t with some random terms, fluctuations of travel time caused by random inhomogeneities can easily be incorporated into the calculations. Thus, the breakdown of the strict modal structure can be simulated. Figure 15 shows the effect of random variations in velocity on phase velocity curves. In this simulation we assumed that the travel time at each angle of incidence was subject to 1% rms. random variation. Notice that the modal structure breaks down even at moderate frequencies and at around 1 Hz most of the modes lose their identity as the phase velocity points become mixed up.

Also, much of the accuracy of modal calculations appears useless because, in a practical sense, inverting $L_g$ data is not possible, and even small perturbations of the models can invalidate detailed comparisons between actual and synthetic seismograms. $L_g$ will always be excited as long as the source is located in the crust and the source depth information is lost in propagation. While the $L_g$ phase can be used to obtain information about major changes in crustal thickness or average crustal velocity, such quantities have little value in discrimination studies.

Decomposition of $L_g$ into distinct modes does not seem feasible because of the modes' similarity in terms of velocity and frequency. Some $L_g$ "phases", group velocity minima, could conceivably be separated several thousand kilometers from the source. However, the crustal structure probably does not remain constant over such distances.

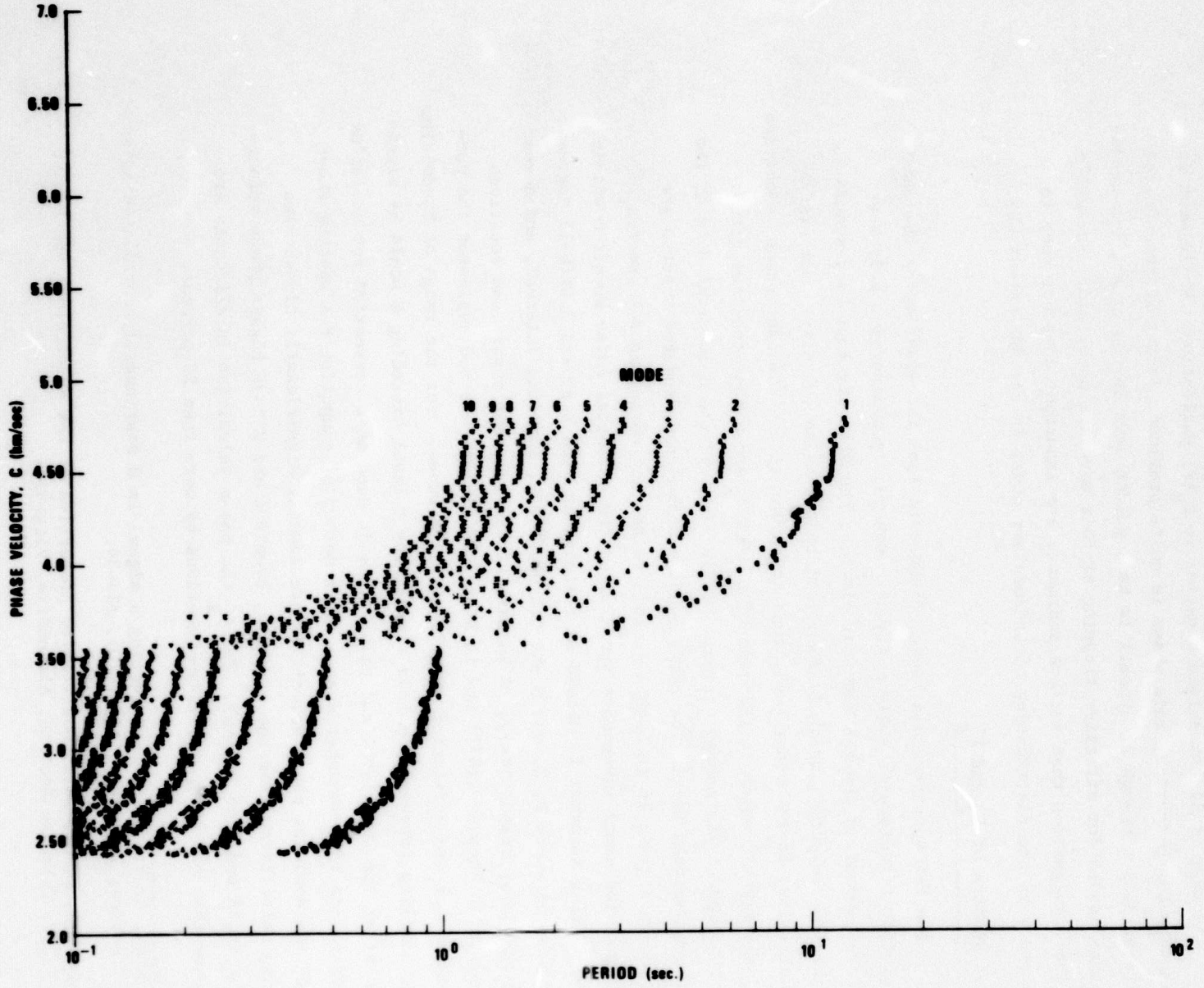


Figure 15. Effect of 1% rms. random variation in the travel times of the phase velocity curves.

Another still unresolved question is $P_g(\overline{P})$ excitation. While weak in Eastern North America, this phase is quite prominent in the Western United States and, although it appears to be a guided wave in the crust, the conditions needed for effective trapping of this wave are uncertain. Haskell's (1966) suggestion that surface sediments are important does not seem to agree with the distribution of sedimentary cover in the EUS versus WUS.

F-K Spectra of $L_g$ and $P_g$

The F-K spectrum is a useful diagnostic tool in establishing the phase velocity structure of a given signal. Coherent nondispersive body wave phases appear on the F-K spectral plots at the velocity that corresponds to the group velocity, which is identical to the phase velocity. Dispersive wavetrains, on the other hand, tend to appear at the dominant phase velocities of the signal, which in the case of $L_g$ and $P_g$ are higher than the group velocities of the energy arrival. Table II gives the epicentral data of the events analyzed here. The corresponding seismograms and F-K spectra are shown in Figures 16 through 21. This method for computing F-K spectra divides the usual wavenumber spectrum by the estimated noise spectrum within the fitting interval to obtain an F-statistic with 2 BT and 2 BT(N-1) degrees of freedom where B, T, and N are the bandwidth, sampling interval, and number of channels, respectively. A summary of the relevant theory and equations appears in Shumway (1971) and in Blandford (1972), who had evaluated the performance of the F-detector on teleseismic P waves. For the range of bandwidths and sampling intervals in this report, any F level exceeding 4 would be significant at the .001 level and this figure is used as a convention for declaring a detection in wavenumber space. This method of computing F-K spectra shows that the dominant phase velocities are usually significantly higher than group velocities. For the $P_g$ phase, Events 1 and 2 have higher phase velocities (6.26 and 6.66 km/sec). For $L_g$ the phase velocities in all cases are higher than the group velocity--sometimes by more than 20 percent.

Shumway, R. H., 1971, On detecting a signal in N stationarily correlated noise series; Technometrics, 10(3), 523-34.

Blandford, R. R., 1972, Qualitative properties of the F-detector; SDL Report 291, Teledyne Geotech, Alexandria, Virginia.

TABLE II

Table of Events

| Event | Date | Origin Time | Coordinates and Region |
|---|---|---|---|
| 1 (113) | 30 Aug 1974 | 19:46:54.0 | 44.6N, 110.765W<br>Hebgen Lake Region, SW Montana |
| 2 (116) | 30 Aug 1974 | 17:01:59.5 | 44.7N, 111.228W<br>Hebgen Lake Region, SW Montana |
| 3 (117) | 30 Aug 1974 | 17:04:45.9 | 44.654N, 111.089W<br>Hebgen Lake Region, SW Montana |
| 4 (114) | 29 May 1973 | 16:06:39.2 | 71.896N, 75.901W<br>Baffin Island Region |
| 5 (118) | 04 Mar 1972 | 12:26:13.0 | 47.813N, 114.379W<br>NW Montana |
| 6 (119) | 04 Mar 1972 | 12:42:04.5 | 47.818N, 114.416W<br>NW Montana |

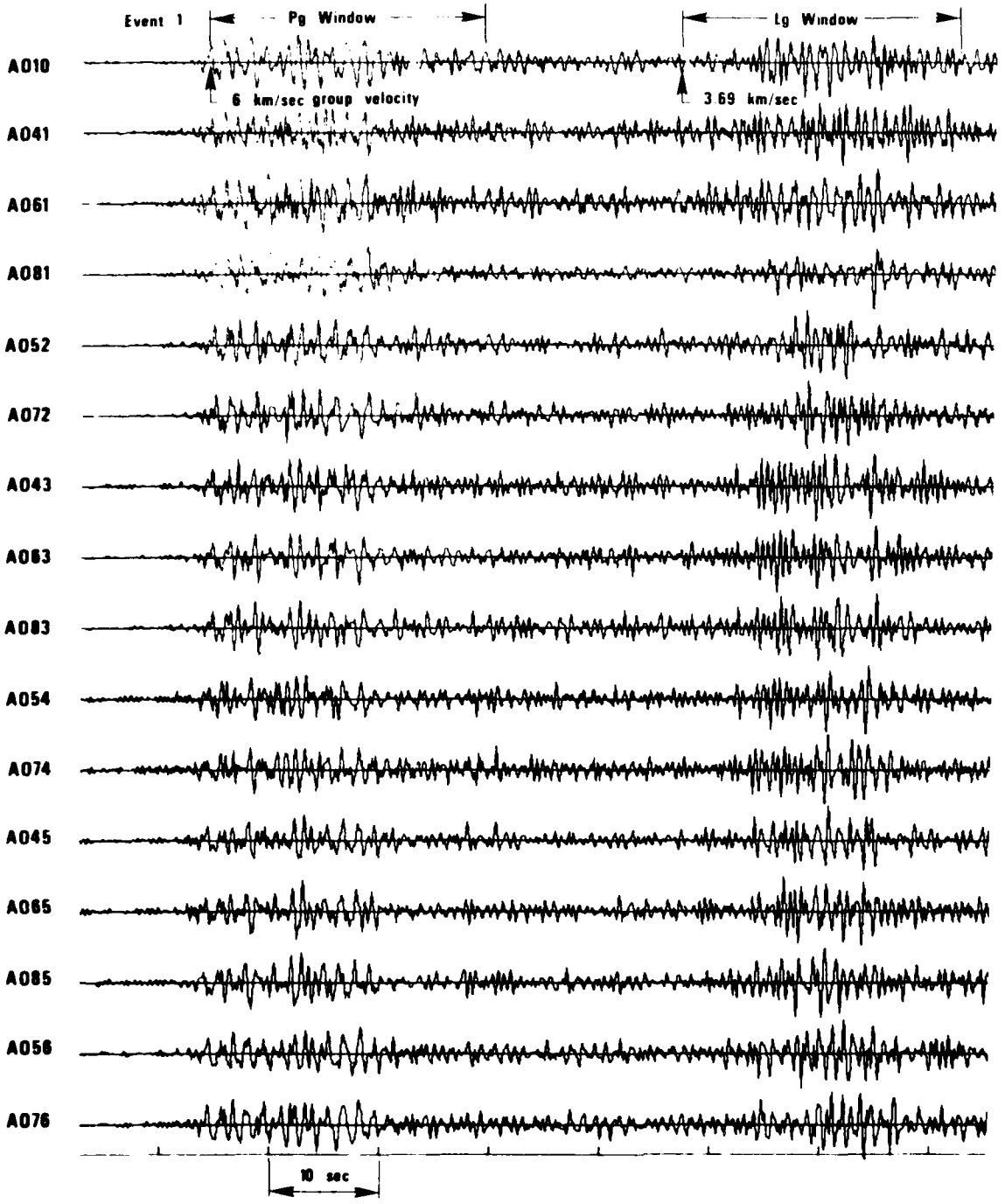


Figure 16a. Event 1, seismogram.

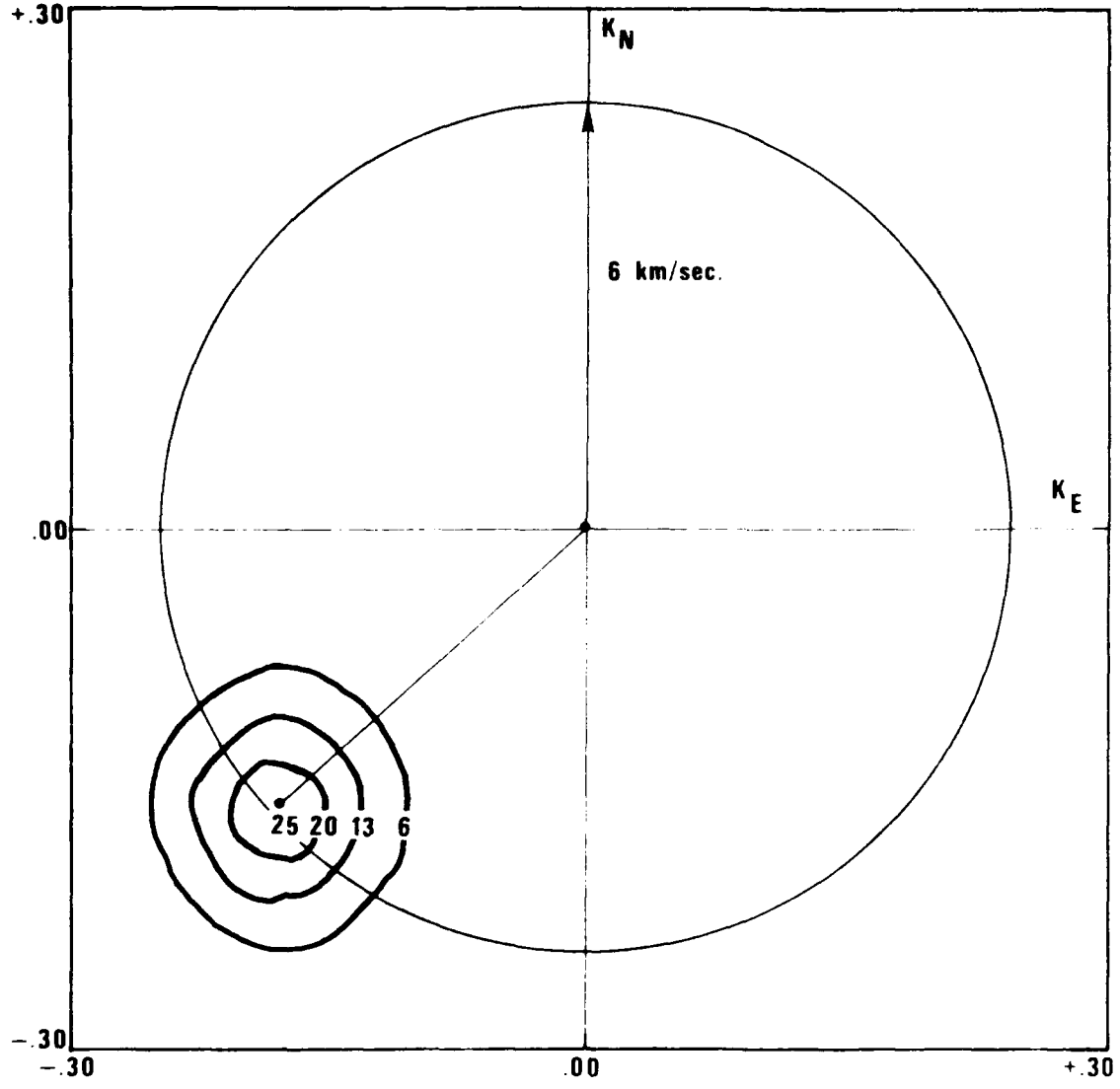


Figure 16b. Event 1, F-wavenumber plot for $P_g$ phase.

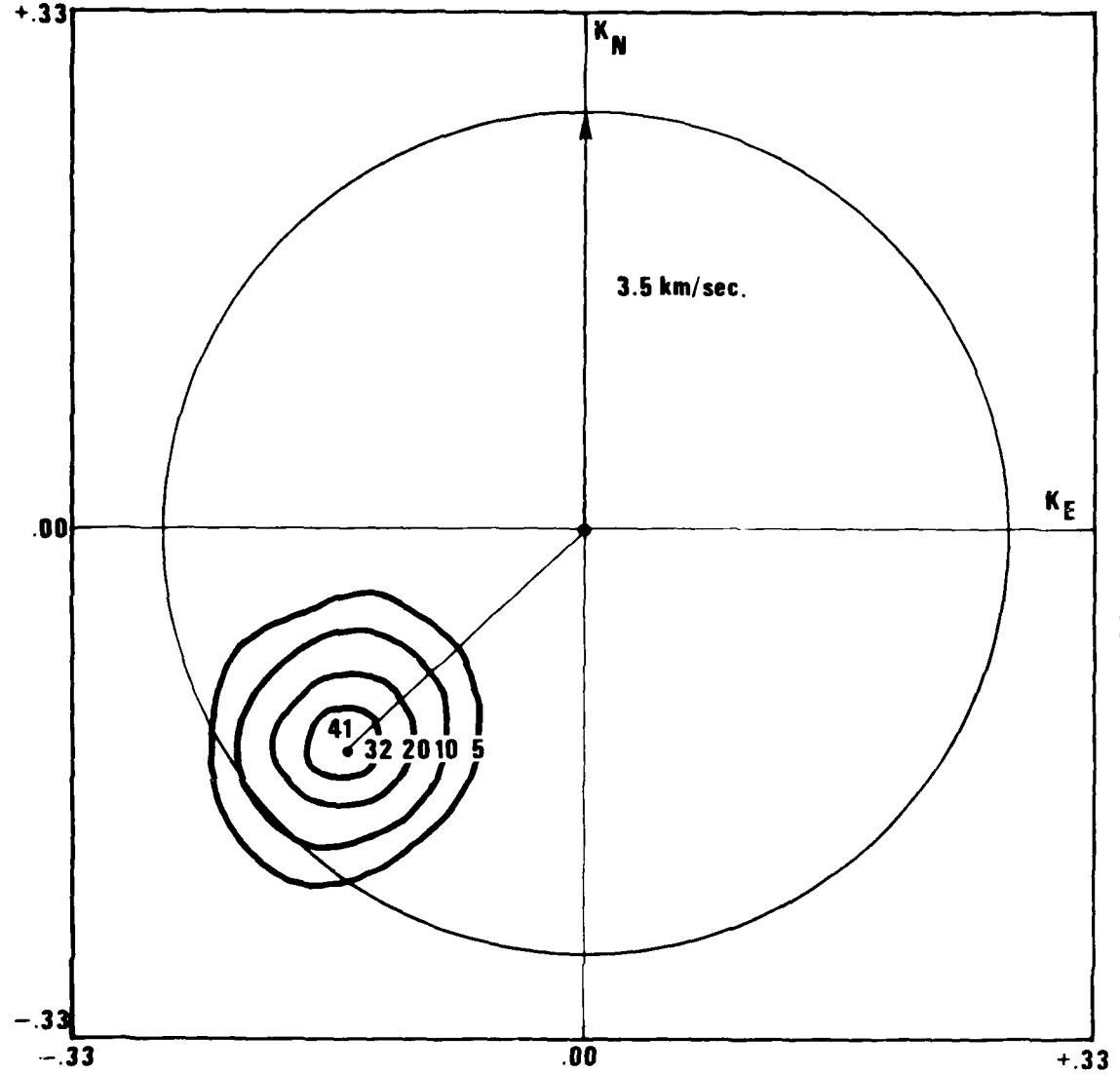


Figure 16c. Event 1, F-wavenumber plot for $L_g$ phase at .94 Hz.

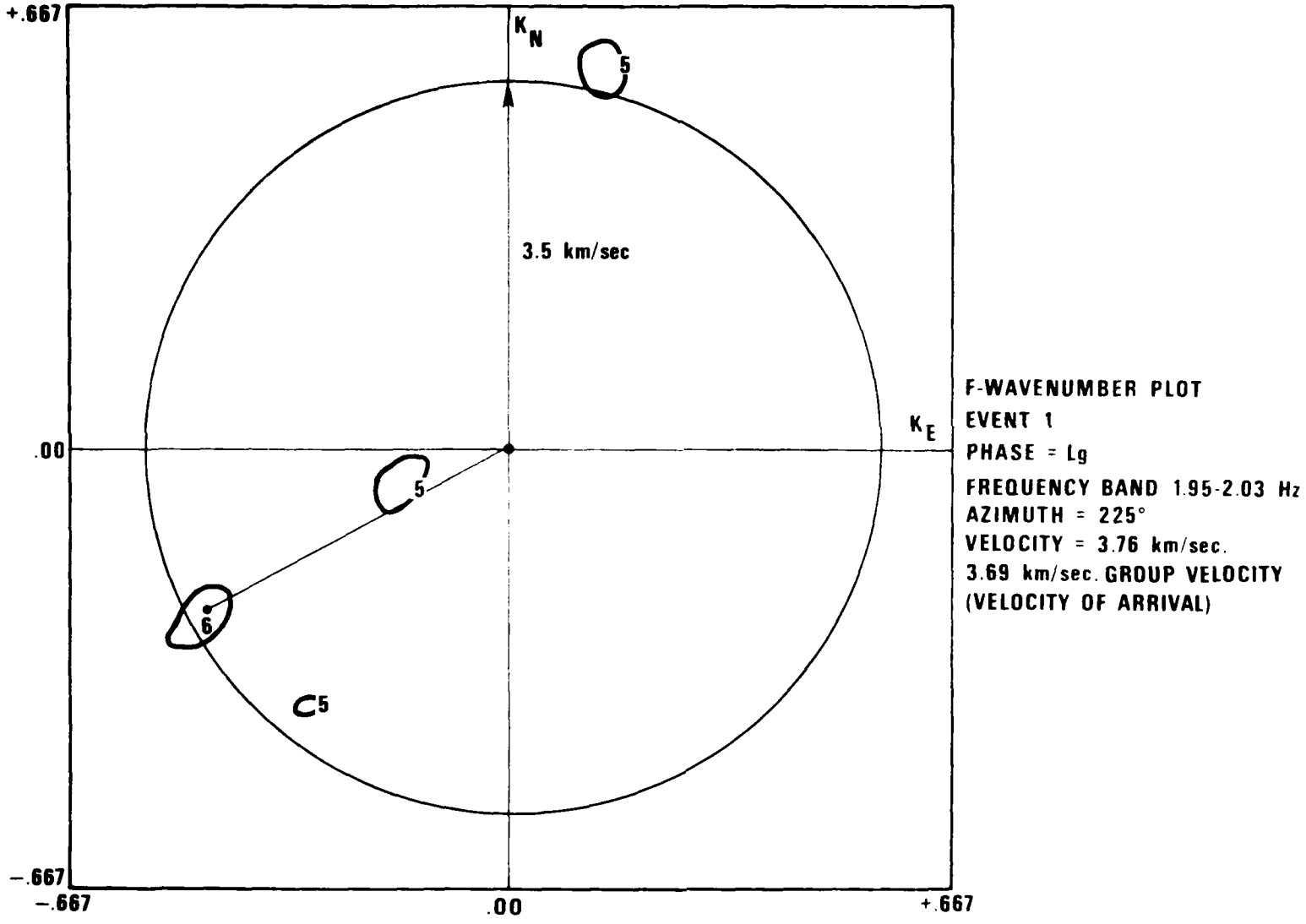


Figure 16d. Event 1, F-wavenumber plot for $L_g$ phase at 1.99 Hz.

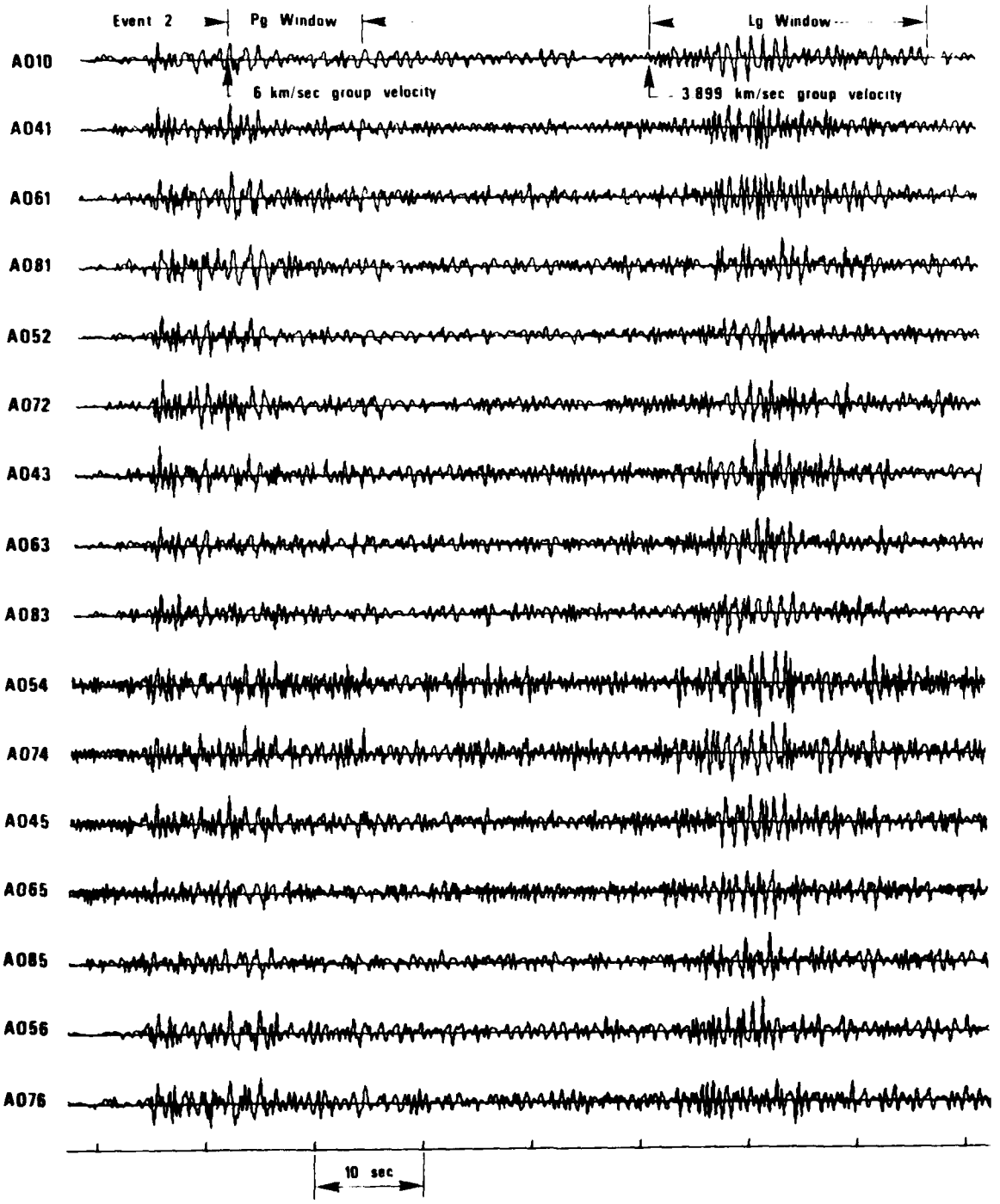


Figure 17a. Event 2, seismogram.

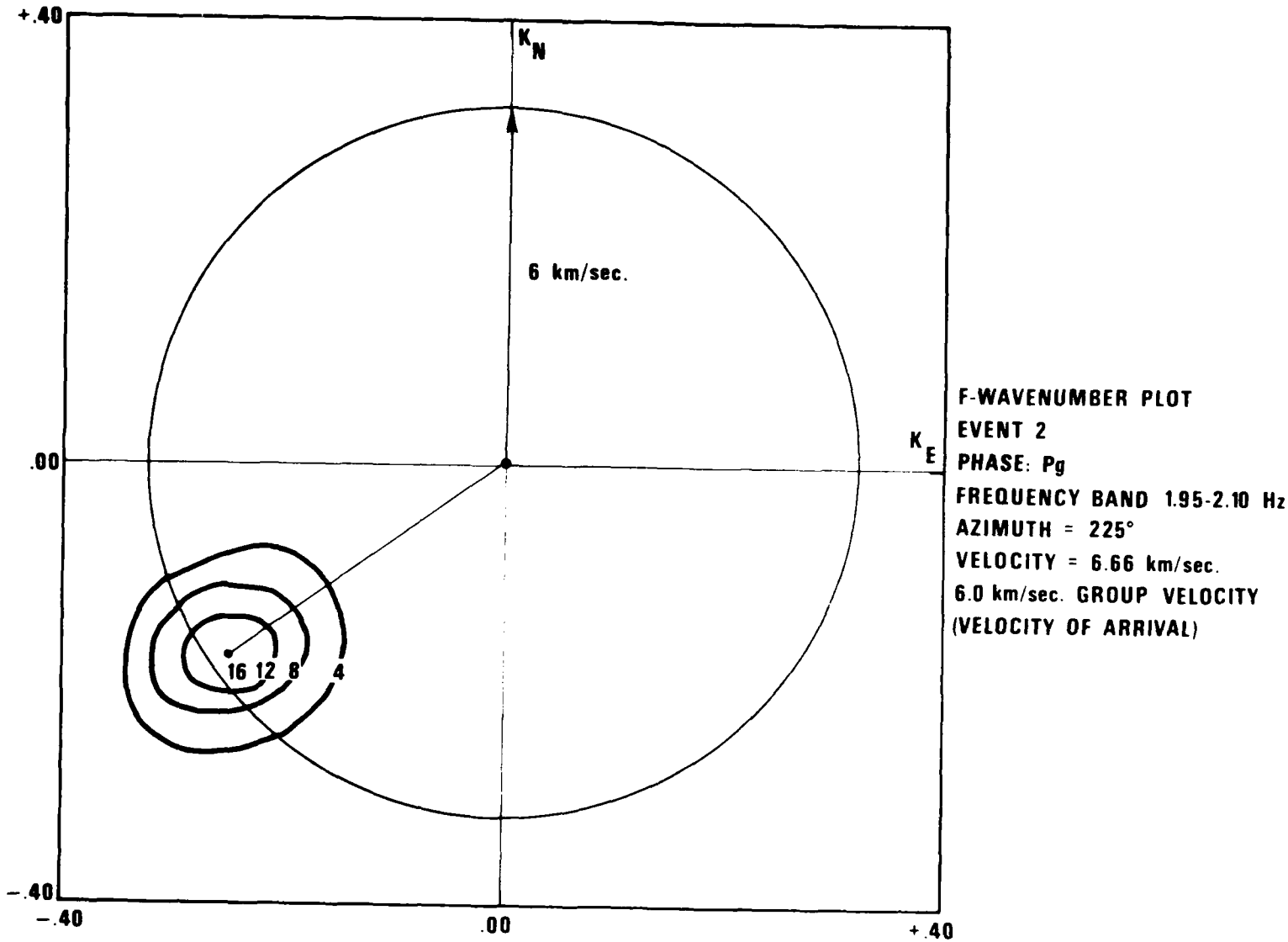


Figure 17b. Event 2, F-wavenumber plot for $P_g$ phase.

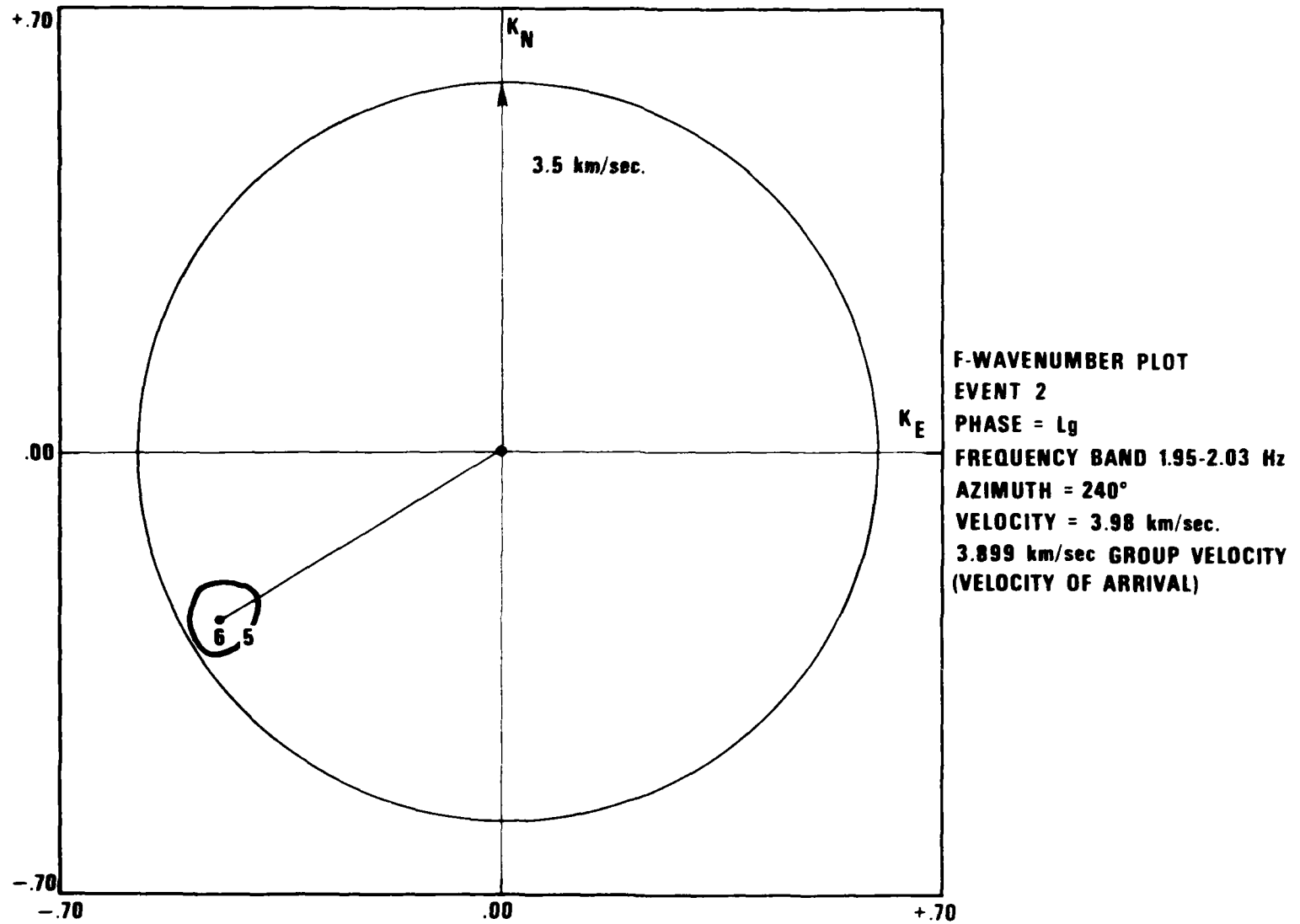




Figure 17c. Event 2, F-wavenumber plot for $L_g$ phase.

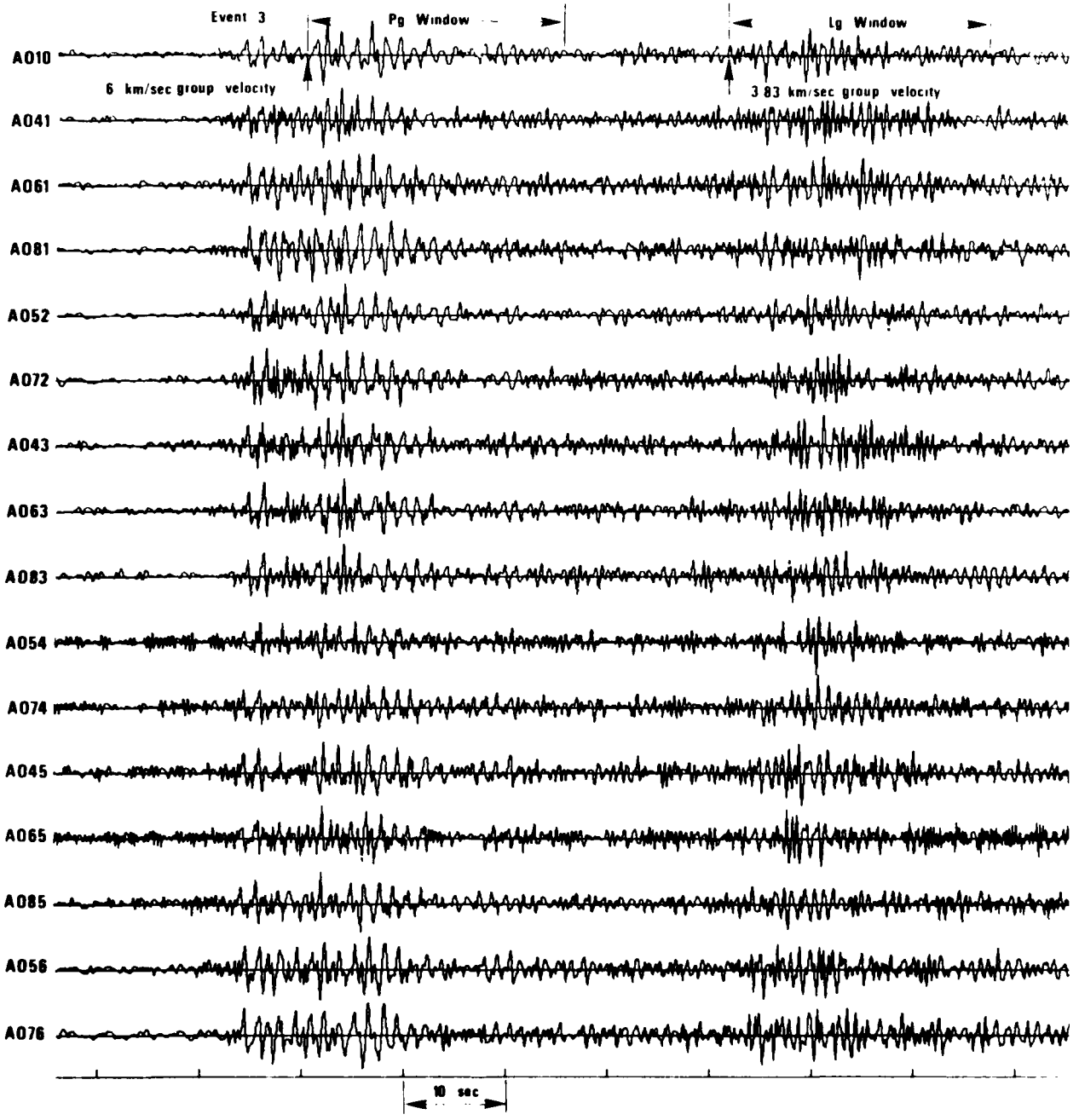


Figure 18a. Event 3, seismogram.

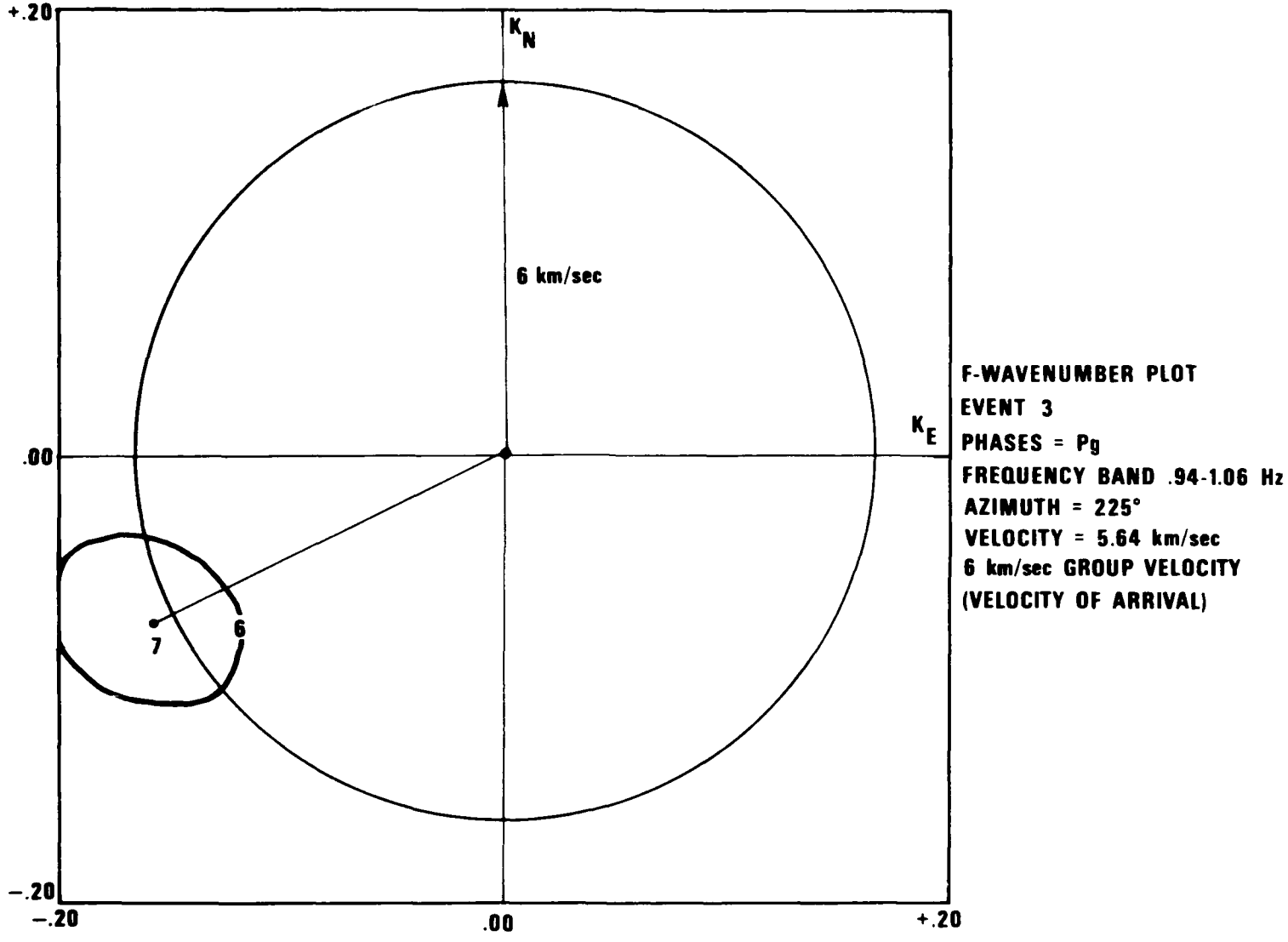


Figure 18b. Event 3, F-wavenumber plot for $P_g$ phase.

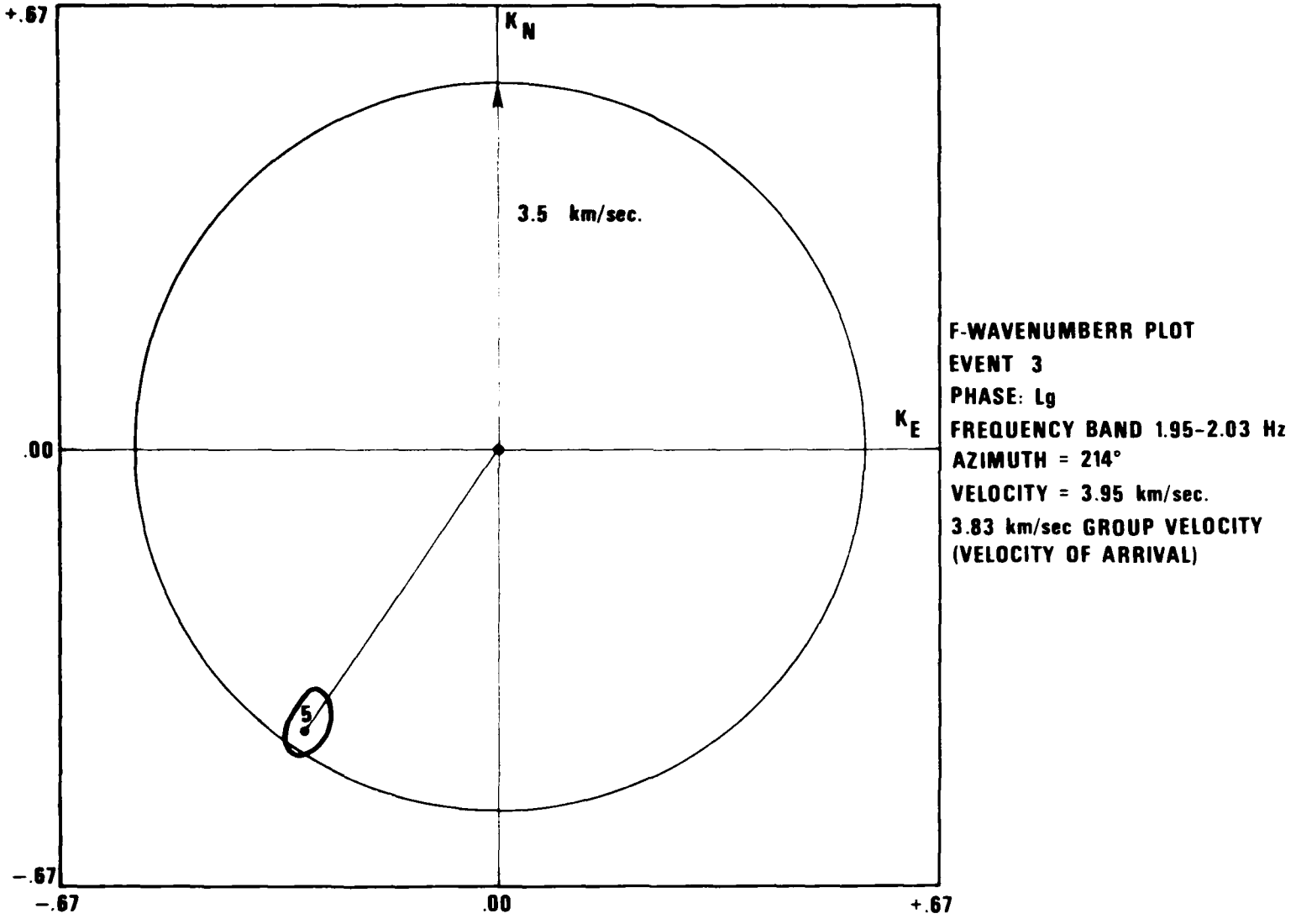


Figure 18c. Event 3, F-wavenumber plot for $L_g$ phase.

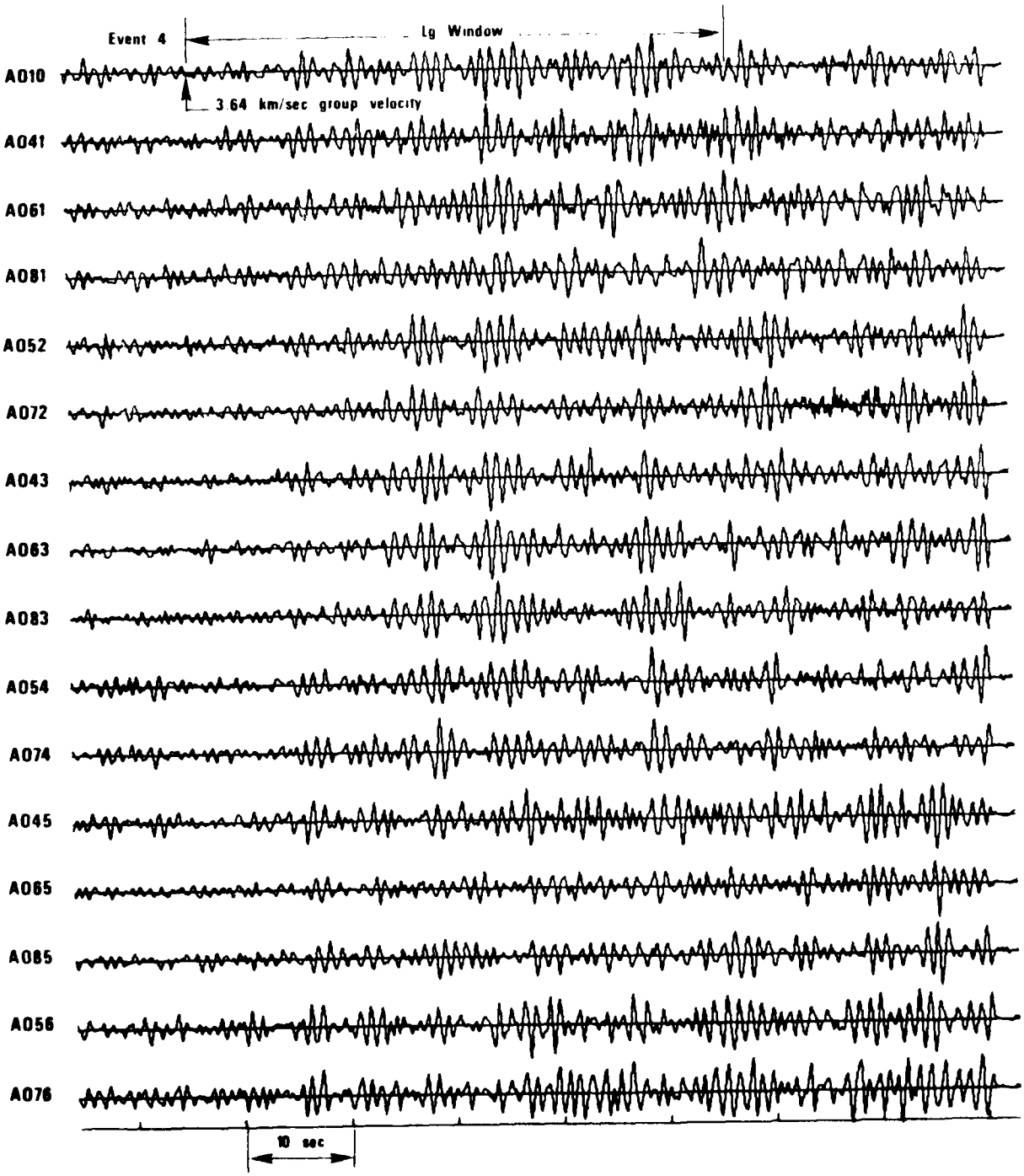


Figure 19a. Event 4, $L_g$ portion of seismogram.

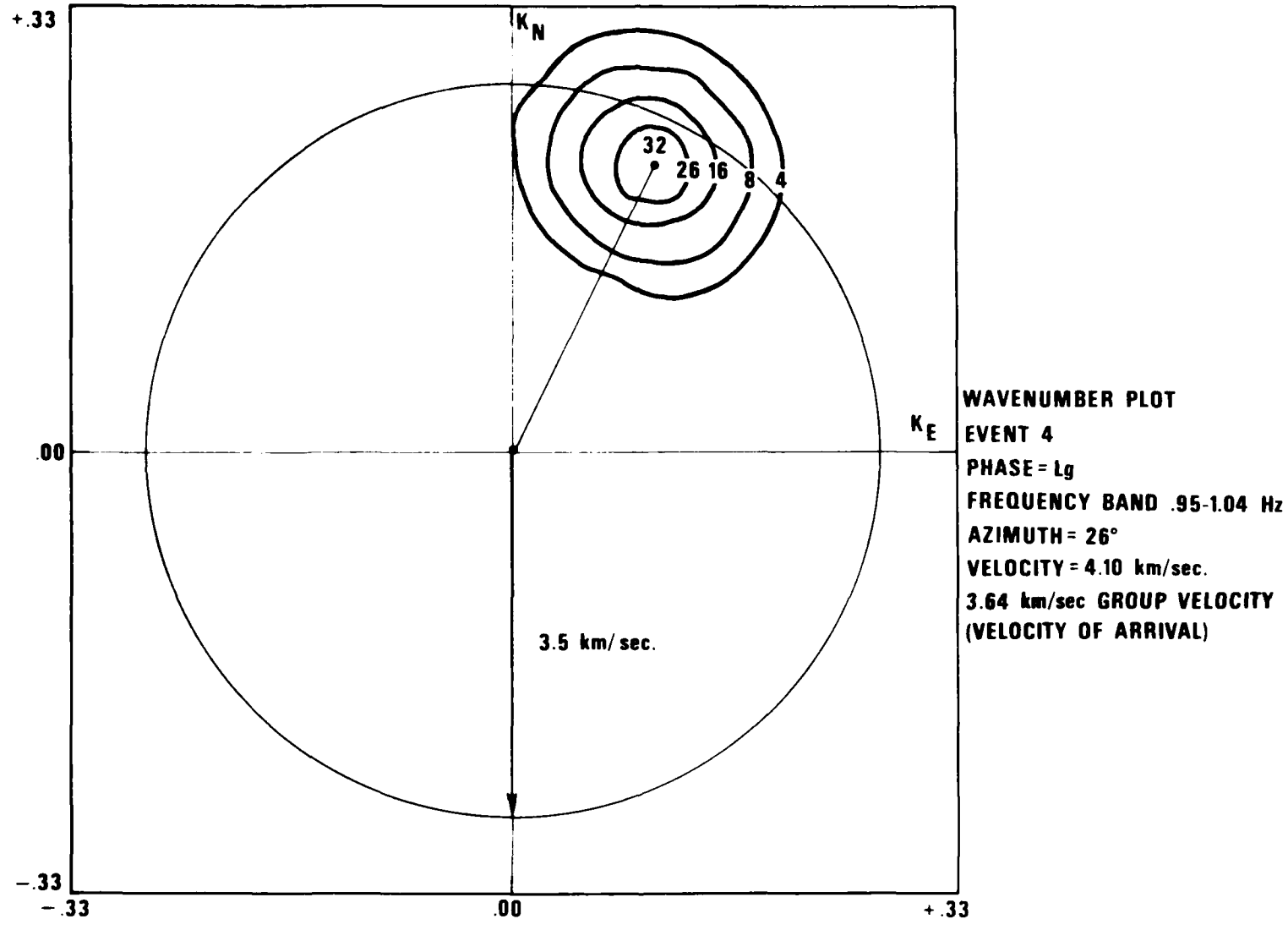


Figure 19b. Event 4, F-wavenumber plot for $L_g$ phase.

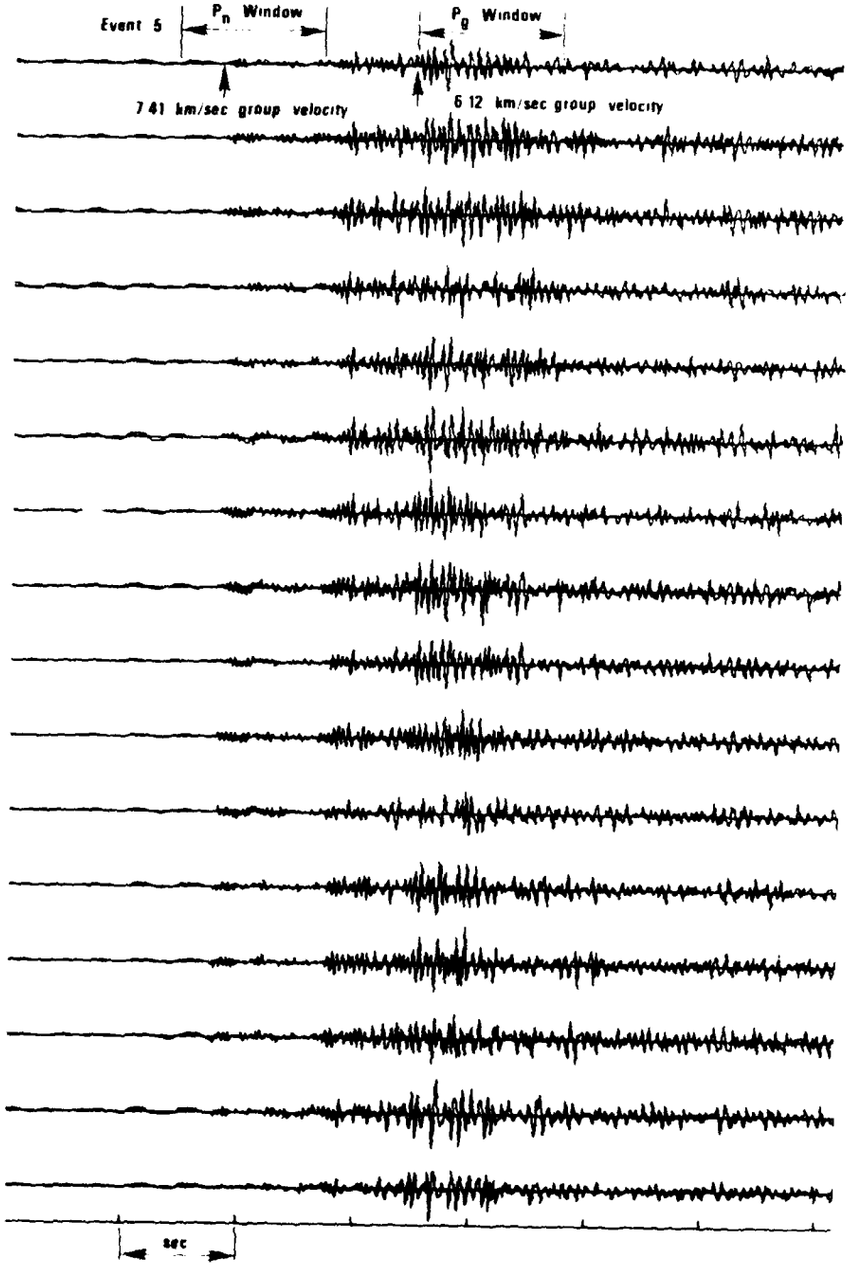


Figure 20a. Event 5, $P_n$ and $P_g$ portions of seismogram.

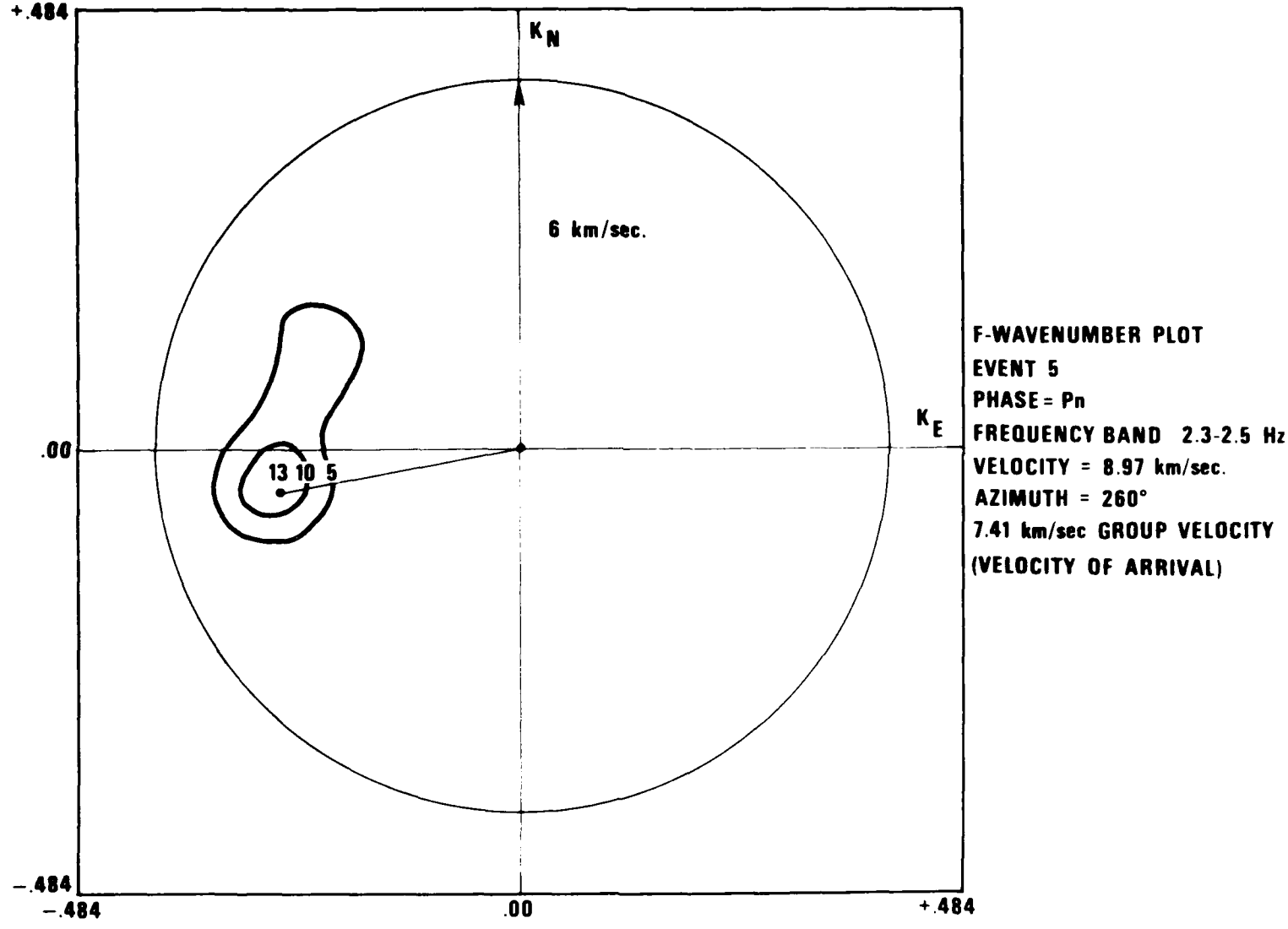


Figure 20b. Event 5, F-wavenumber plot for $P_n$ phase.

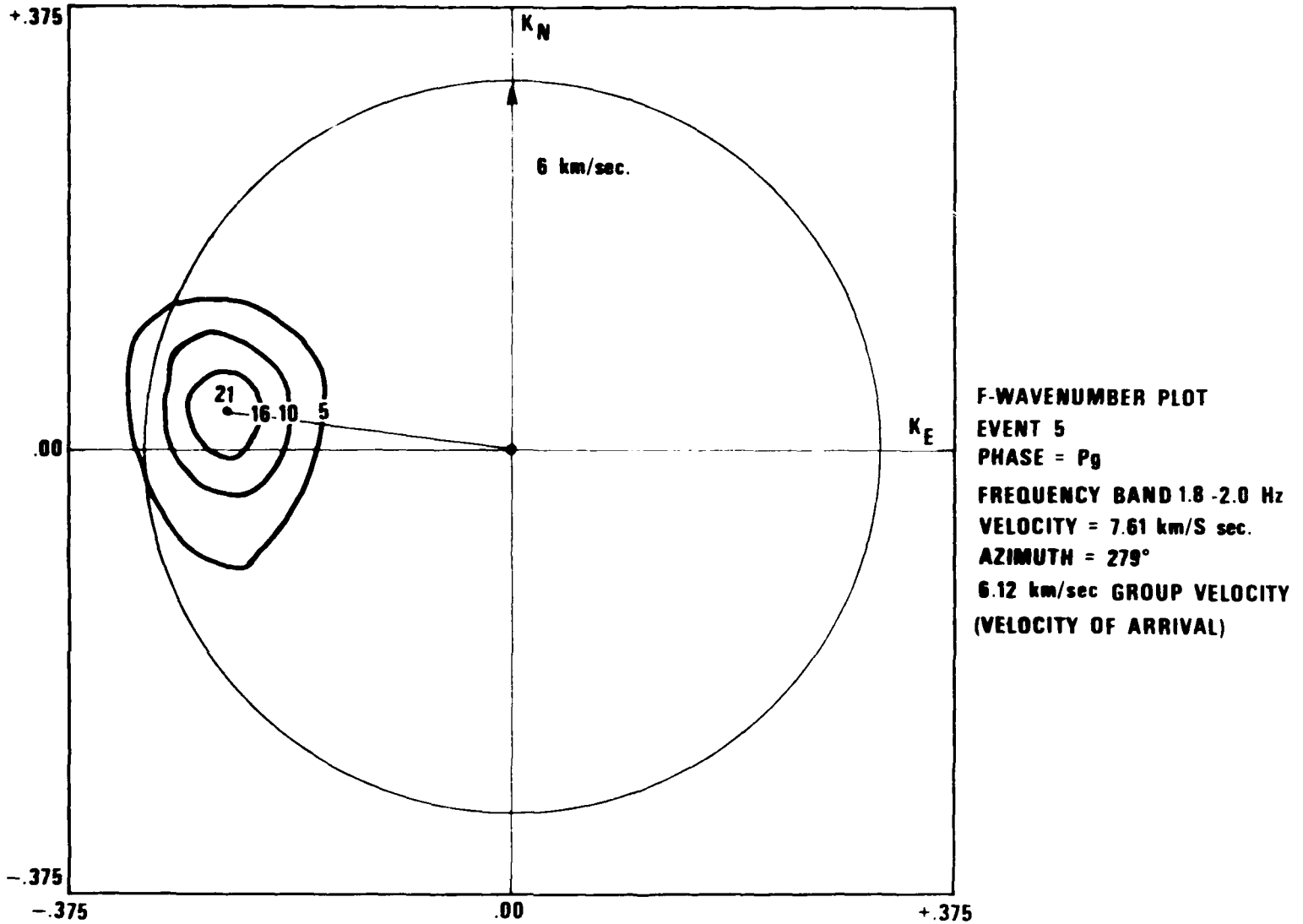




Figure 20c. Event 5, F-wavenumber plot for $P_g$ phase.

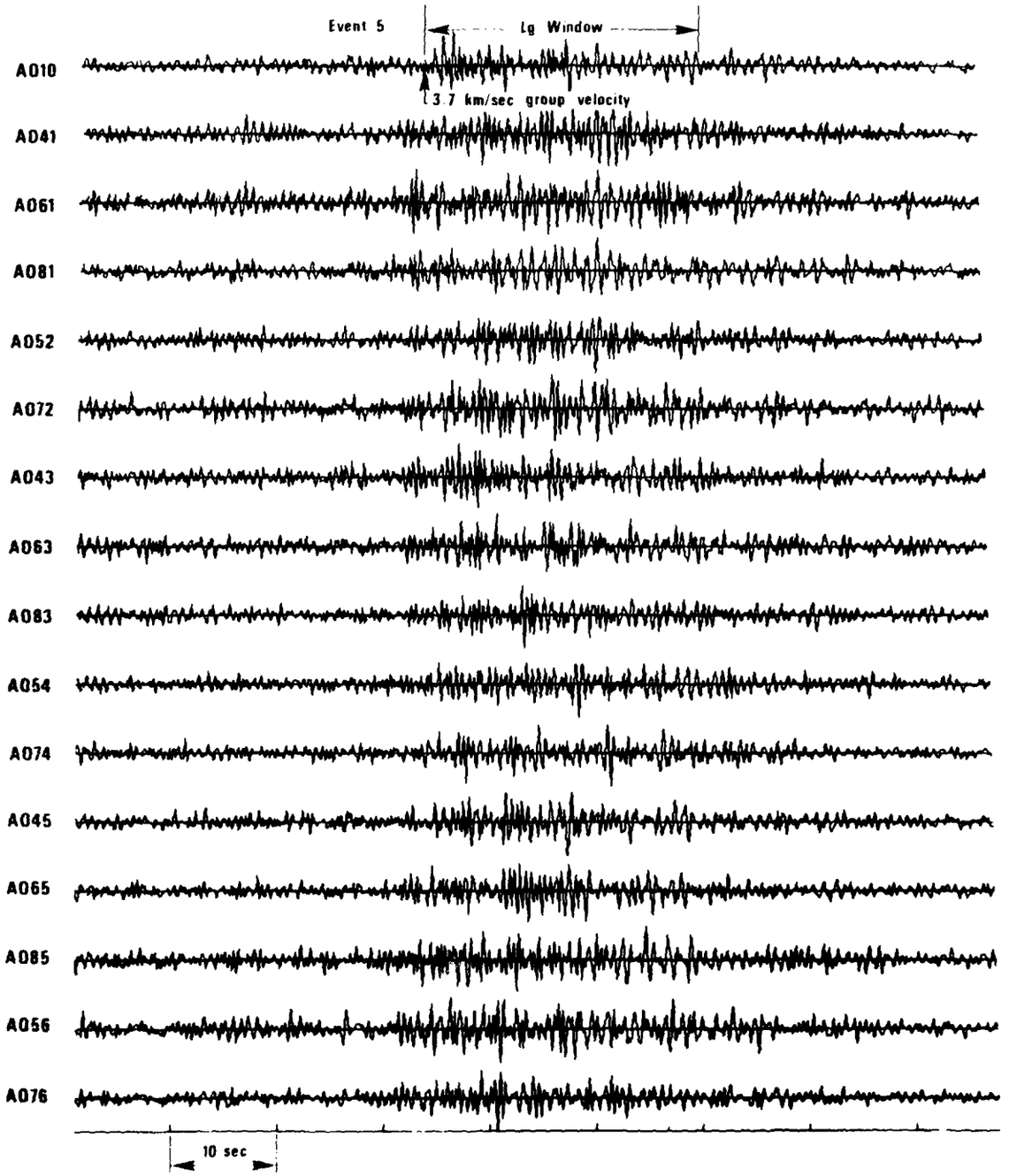


Figure 20d. Event 5, $L_g$ portion of seismogram.

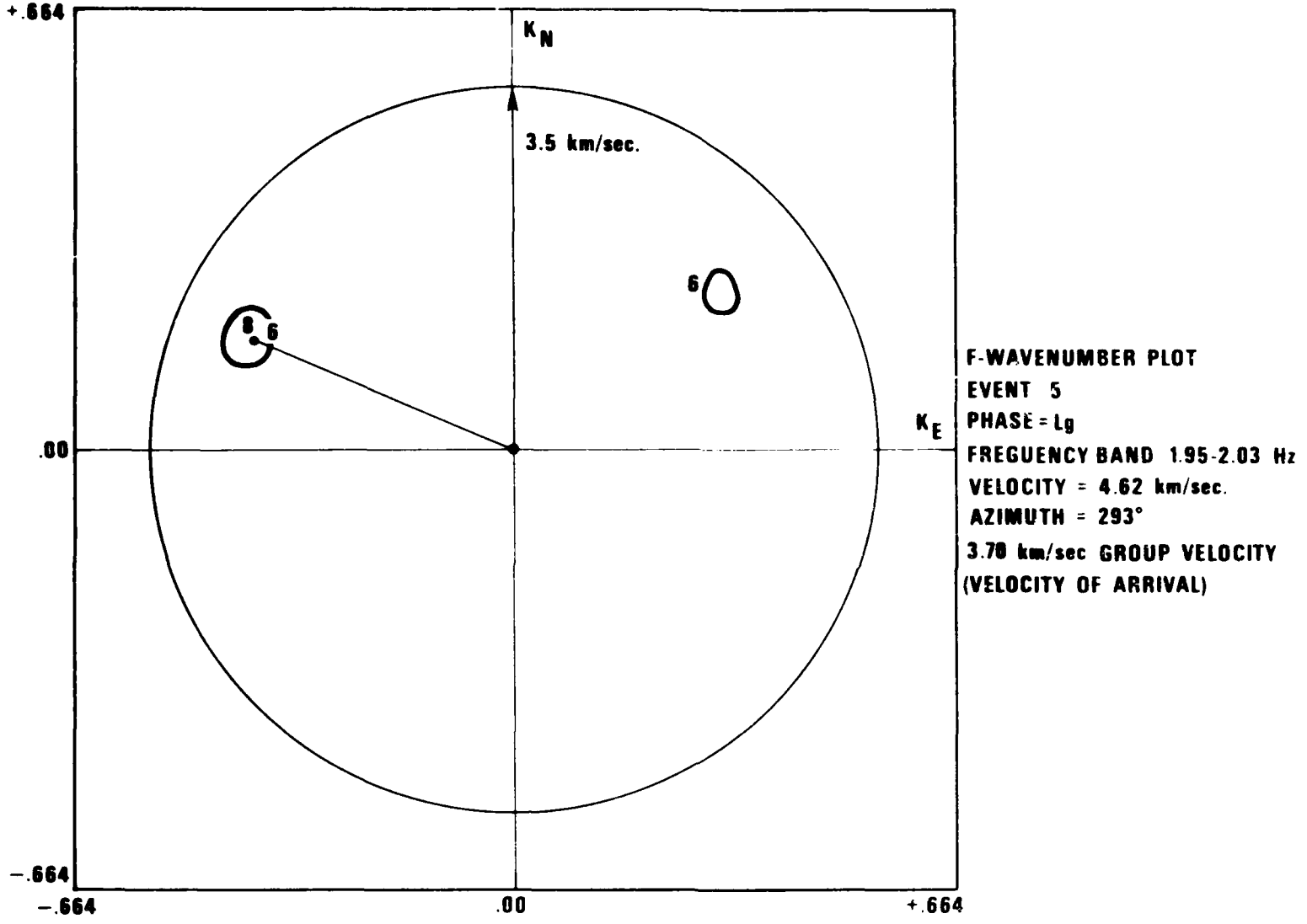


Figure 20e. Event 5, F-wavenumber plot for $L_g$ phase.

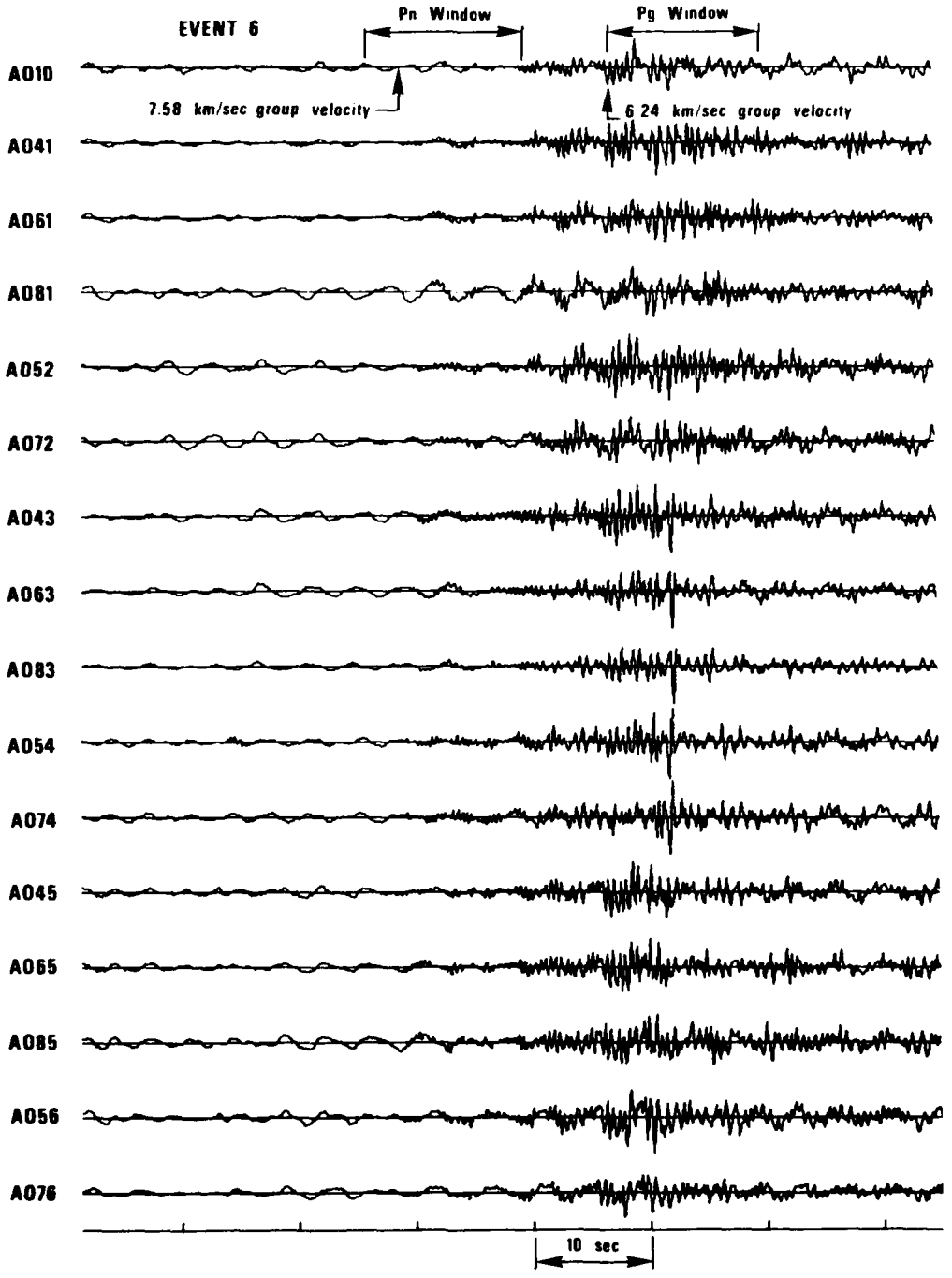


Figure 21a. Event 6, $P_n$ and $P_g$ portions of seismogram.

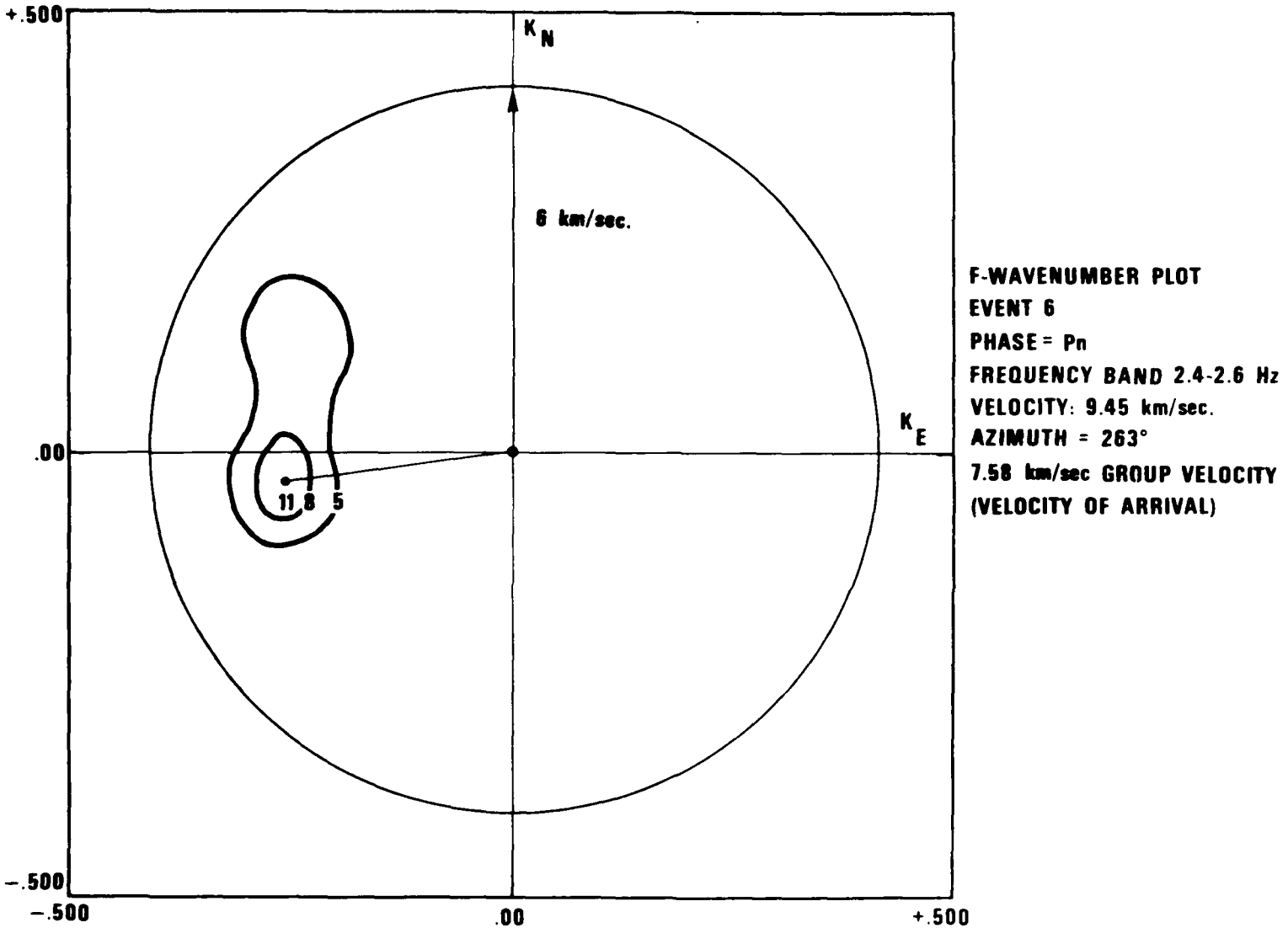


Figure 21b. Event 6, F-wavenumber plot for $P_n$ phase.

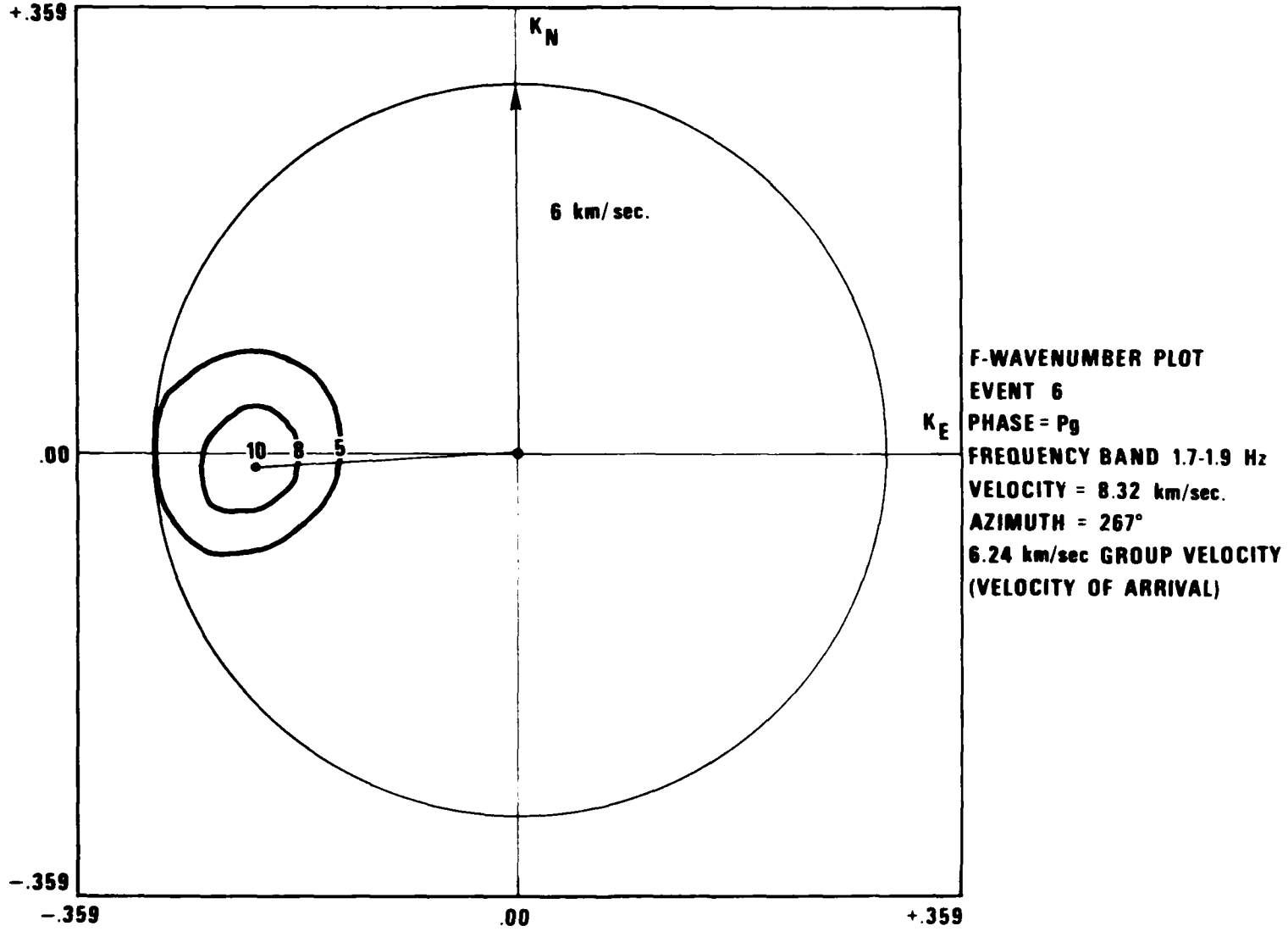


Figure 21c. Event 6, F-wavenumber plot for $P_g$ phase.

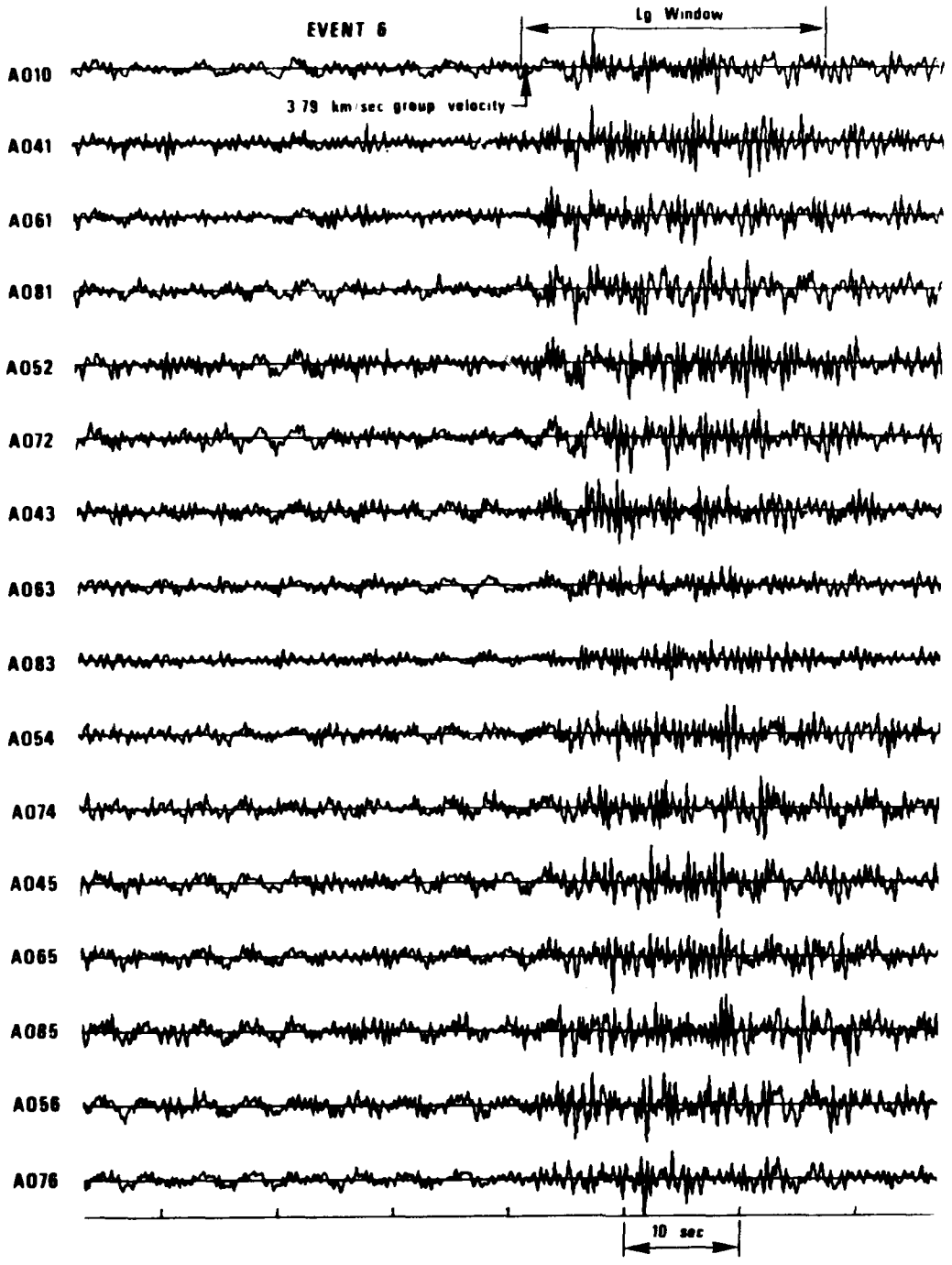


Figure 21d. Event 6, $L_g$ portion of seismogram.

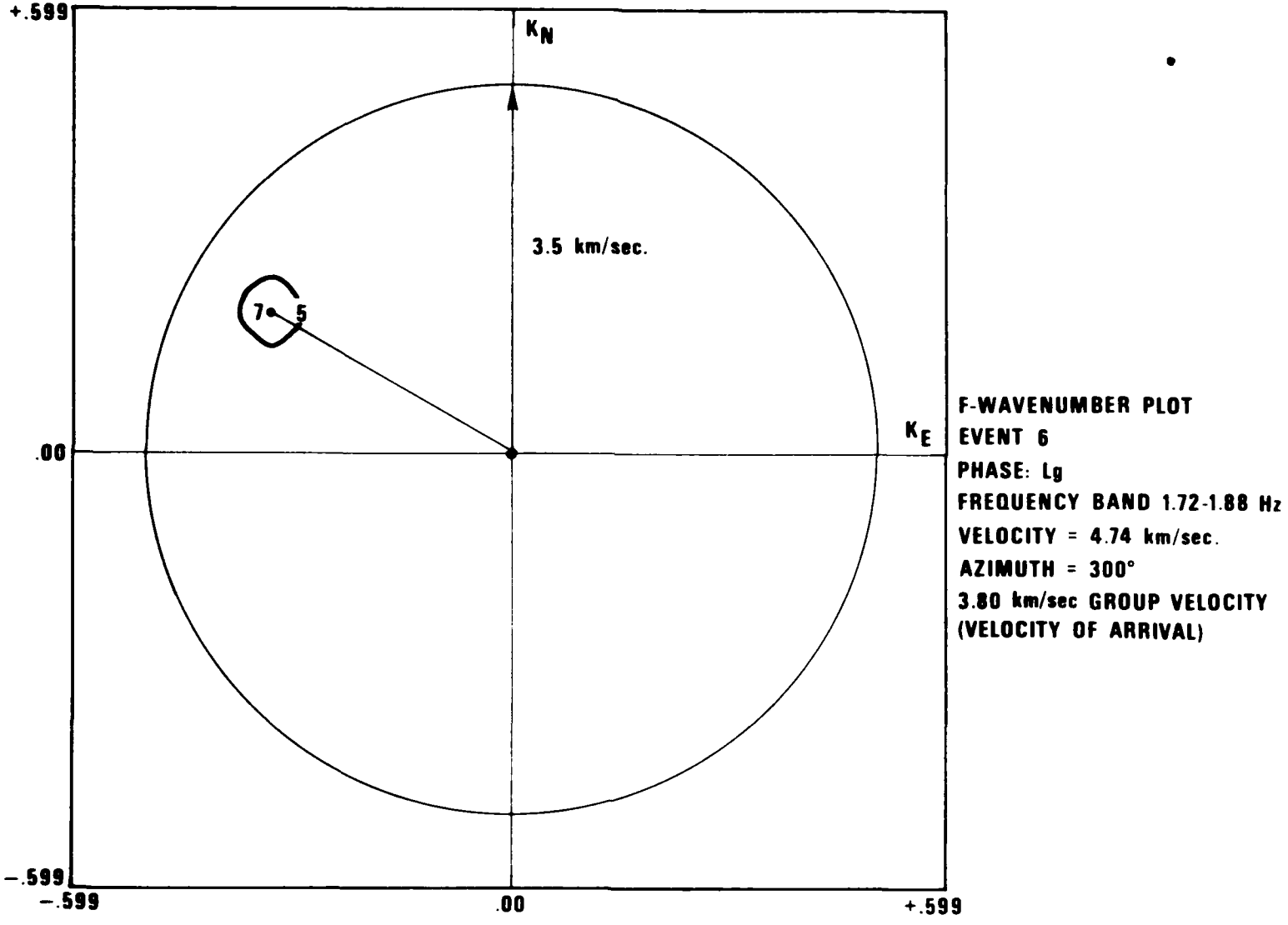


Figure 21e. Event 6, F-wavenumber plot for $L_g$ phase.

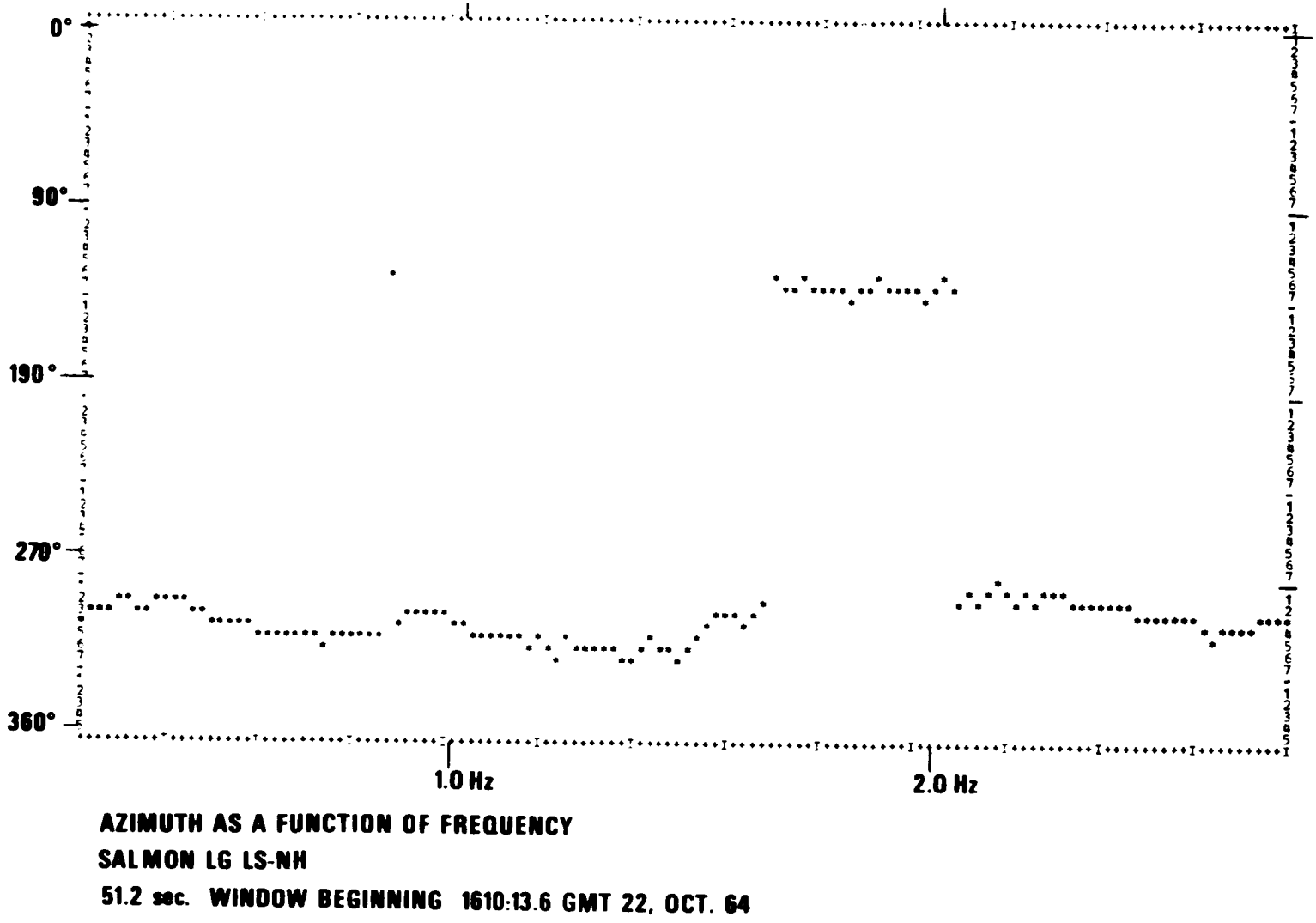


Figure 22. Apparent azimuth of arrival of Salmon $L_g$ phase at station LS-NH.

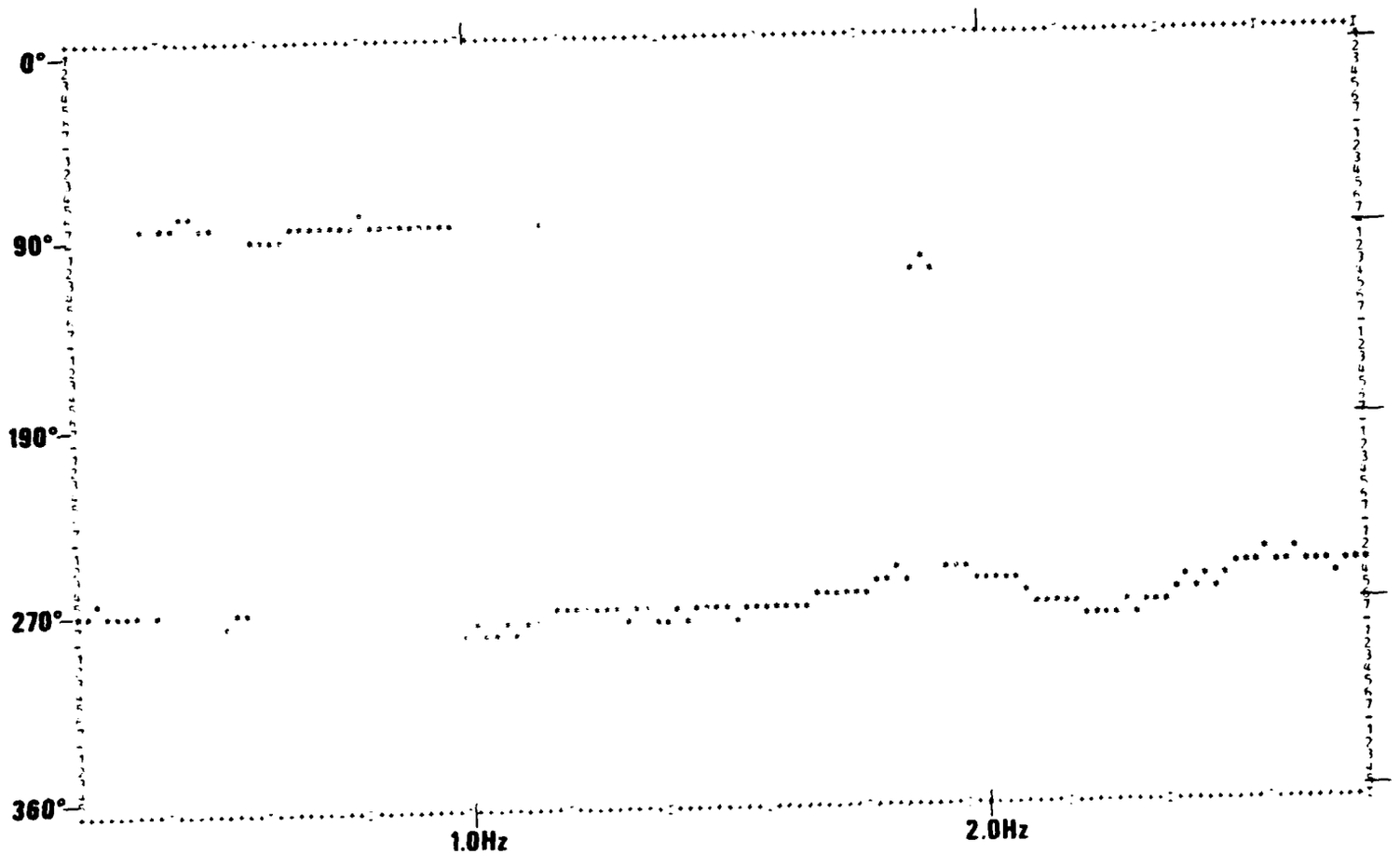


Figure 23. Apparent azimuth of arrival of Gnome $P_g$ phase at station DR-CO.

For Events 5 and 6, all phase velocities are more than 20% greater than the corresponding group velocity, a figure including $P_n$, $P_g$, and $L_g$ phases. In fact, one important conclusion of this work is that beaming velocity varies for these phases. This occurs because the modal composition at a given frequency varies among events. Because the modes cannot be separated at moderate distances (the basic limitation is the uncertainty principle), interpreting these changes does not appear feasible. Any detector using beaming, therefore, should use a range of beam velocities for the regional phases $P_g$, $(\bar{P})$ and $L_g$.

Particle Motion

Like the F-K spectra, Smart's (1977) detector can also diagnose the modal structure. Rayleigh waves have typically elliptical particle motion that can be either prograde or retrograde, depending upon the mode number and frequency range. Higher modes usually have a high ellipticity; that is, they have a small ratio of horizontal to vertical displacement. Similarly, the leaky modes that make up the $P_g$ wavetrain also have elliptical particle motion that can be either retrograde or prograde. Although originally designed for fundamental modes, Smart's surface wave processor also performs well on $L_g$ (Smart, 1977). The direction of arrival determination of the processor is based upon retrograde motion; if run on waves with prograde orbital motion the azimuth determined will be off by 180°. Figure 22 shows the azimuth of arrival from surface wave detection as a function of frequency. Input to the program was the $L_g$ wavetrain from the nuclear explosion SALMON at the LRSM station LSNH. The 180° shifts in azimuth at about 1.6 and 2 Hz reveal the frequencies where prominent motion changes from prograde to retrograde. Probably, both types of particle motion are present at each frequency in the various modes, partially cancelling each other and degrading the effectiveness of the processor.

Figure 23 shows a printer plot for a $P_g$ phase at station DRCO from the GNOME nuclear explosion. Changes from prograde to retrograde motion,

Smart, E., 1977, A three-component single-station maximum-likelihood surface wave processor; SDAC-TR-77-14, Teledyne Geotech, Alexandria, Virginia.

characteristic of leaky modes making up this wavetrain (Su and Dorman, 1965; Haskell, 1966), are evident. The ellipticity of particle motion alone does not prove that either $P_g$ or $L_g$ are superpositions of modes, because P and SV waves incident on a layered medium bounded by a free surface also produce elliptical motion (Nuttli, 1964).

Su, S. S. and J. Dorman, 1965, The use of leaking modes in seismogram interpretation and in studies of crust-mantle structure; Bull. Seism. Soc. Am., 55, 989.

Nuttli, O., 1964, The determination of S-wave polarization angles for an earth model with crustal layering; Bull. Seism. Soc. Am., 54, 1429.

## CONCLUSIONS

The modal and spatial coherence structure of $L_g$ and $P_g$ can be effectively simulated using ray tracing and Brune's (1964) modal interference criterion.

For arrays of moderate size (D ≃ 10 km), the $P_g$ and $L_g$ phases should remain fairly coherent, even if all possible modes are excited.

The higher modes are extremely sensitive to topography and to random velocity variations in the crustal wave guide. Minor surface roughness and small random variations in the velocity cause extensive mode conversion and breakdown of mode structure. For high frequencies, simulations using normal modes in flat layered structures are not realistic and do not possess significant detail above a statistical level.

Because of probable mode conversions, much of the source depth information in the crust is lost in $P_g$ and $L_g$.

To effectively simulate short period $P_g$ and $L_g$ phases, a stochastic theory is needed like that in the scattering theory of lunar seismograms; that is, merely an attempt to predict the amplitude envelope and frequency content of these phases. Modal theory is strictly applicable only to the low frequency range of each mode (F < .5 Hz), although modal interference criteria may still govern local motion.

The F-K spectra tend to give velocities higher than group velocity (energy arrival velocity) of each phase, suggesting that $P_g$ and $L_g$ propagate at least locally as dispersive normal modes; these phases should be beamed at those higher velocities. Because of modal composition variation among events a single fixed beam velocity for each phase would not be efficient.

Particle motion of $P_g$ and $L_g$ phases has an alternating prograde-retrograde character as a function of frequency, in accordance with the presumed modal composition. This property can be exploited for detection and source location.

## ACKNOWLEDGEMENTS

The authors thank Dr. Robert Shumway who helped to perform the F-K calculations and Dr. B. R. Julian for giving us his computer program, TVT2, for raytracing.

## REFERENCES


Backus, G. E. and J. F. Gilbert, 1970, Uniqueness in the inversion of gross earth data; Phil Trans. R. Soc. Lond., No. 266, 123.

Ben-Menahem, A, 1964, Mode-ray duality; Bull. Seism. Soc. Am , 54, 1315.

Bessonova, E. N., V. M. Fishman, V. Z. Ryoboyi, G. A. Sitnikova, 1974, The tau method for inversion of travel times - I, Deep seismic sounding data; Geophys. J. R. Astr. Soc., 36, 377.

Blandford, R. F , 1972, Qualitative properties of the F-detector; Seismic Data Laboratory Report 291, Teledyne Geotech, Alexandria, Virginia.

Brune, J. N., 1964, Travel times, body waves and normal modes of the Earth; Bull. Seism. Soc. Am., 54, 2099-2128.

Brune, J. N., 1966, P and SV wave travel times and spheroidal normal modes of a homogeneous sphere; J. Geophys. Res., 71, 2959.

Haskell, N. A., 1966, The leakage attenuation of continental crustal P waves; J. Geophys. Res., 71, 9355.

Johnson, L. E. and F. Gilbert, 1972, A new datum for use in the body wave travel time inverse problem; Geophys. J. R. Astr. Soc., 30, 373.

Julian, Bruce R. and Don L. Anderson, 1968, Travel times, apparent velocities and amplitudes of body waves; Bull. Seism. Soc. Am., 58, 339.

Knopoff, L., F. Schwab, E. Kausel, 1973, Interpretation of $L_g$, Geophys. J. R. Astr. Soc., 33, 389.

Knopoff, L., F. Schwab, K. Nakanichi and F. Chang, 1974, Evaluation of $L_g$ as a discriminant among different continental crustal structures; Geophys. J. R. Astr. Soc., 39, 41.

Langston, C. A. and D. V. Helmberger, 1974, Interpretation of body and Rayleigh waves from NTS to Tucson, Bull. Seism. Soc. Am., 64, 1919.

Mack, H. and E. A. Flinn, 1971, Analysis of the spatial coherence of short-period acoustic gravity waves in the atmosphere; Geophys. J. R. Astr. Soc., 26, 255.

Nuttli, O., 1964, The determination of S-wave polarization angles for an earth model with crustal layering; Bull. Seism. Soc. Am., 54, 1429.

Panza, G. F. and G. Calcagnile, 1975, $L_g$, $L_i$ and $R_g$ from Rayleigh modes; Geophys. J. R. Astr. Soc., 40, 475.

Panza, G. F., F. Schwab and L. Knopoff, 1972, Crustal and channel Rayleigh waves; Geophys. J. R. Astr. Soc., 30, 273.

Press, F. and M. Ewing, 1952, Two slow surface waves across North America; Bull. Seism. Soc. Am., 43, 219.

Ruzaikin, A. I., I. L. Nersesov, V. I. Khatturin and P. Molnar, 1977, Propagation of $L_g$ and lateral variations in crustal structures in Asia; J. Geophys. Res., 82, 307.

Schwab, F., E. Kausel and L. Knopoff, 1974, Interpretation of $S_a$ for a shield structure; Geophys. J. R. Astr. Soc., 36, 737.

Shumway, R. H., 1971, On detecting a signal in N stationarily correlated noise series; Technometrics, 10(3), 523-34.

Smart, E., 1977, A three-component single-station maximum-likelihood surface wave processor; SDAC-TR-77-14, Teledyne Geotech, Alexandria, Virginia.

Su, S. S. and J. Dorman, 1965, The use of leaking modes in seismogram interpretation and in studies of crust-mantle structure; Bull. Seism. Soc. Am., 55, 989.

Tolstoy, I. and C. S. Clay, 1966, Ocean Acoustics: New York, McGraw Hill Book Co.

Vered, M. and A. Ben-Menahem, 1974, Application of synthetic seismograms to the study of low magnitude earthquakes in the northern Red Sea region; Bull. Seism. Soc. Am., 64, 1221.